Received: 17 May 2023 | Revised: 5 February 2024 | Accepted: 21 February 2024

DOI: 10.1002/elsc.202300211

Engineering in Life Sciences

REVIEW

Current trends in medium-chain-length polyhydroxyalkanoates: Microbial production, purification, and characterization

Thomas Hahn[1] | **Melissa Ortega Alzate**[1,2] | **Steven Leonhardt**[1] | **Pravesh Tamang**[1] | **Susanne Zibek**[1,3]

[1]Bioprocess Development, Fraunhofer Institute for Interfacial Engineering and Biotechnology IGB, Stuttgart, Germany

[2]Department of Chemical Engineering, University of Antioquia, El Carmen de Viboral, Colombia

[3]Institute of Interfacial Engineering and Plasma Technology IGVP, University of Stuttgart, Stuttgart, Germany

Correspondence
Thomas Hahn, Bioprocess Development, Fraunhofer IGB, Nobelstraße 12, 70569 Stuttgart, Germany.
Email: thomas.hahn@igb.fraunhofer.de

Funding information
Ministerium für Umwelt, Klima und Energiewirtschaft Baden-Württemberg / Europäische Union (EU), Grant/Award Number: 2076393; Bundesministerium für Bildung und Forschung (BMBF), Grant/Award Numbers: 031B0371A, 031B0371D; Bundesministerium für Ernährung und Landwirtschaft (BMEL), Grant/Award Number: 2221NR012B

Abstract

Polyhydroxyalkanoates (PHAs) have gained interest recently due to their biodegradability and versatility. In particular, the chemical compositions of medium-chain-length (mcl)-PHAs are highly diverse, comprising different monomers containing 6–14 carbon atoms. This review summarizes different feedstocks and fermentation strategies to enhance mcl-PHA production and briefly discusses the downstream processing. This review also provides comprehensive details on analytical tools for determining the composition and properties of mcl-PHA. Moreover, this study provides novel information by statistically analyzing the data collected from several reports on mcl-PHA to determine the optimal fermentation parameters (specific growth rate, PHA productivity, and PHA yield from various structurally related and unrelated substrates), mcl-PHA composition, molecular weight (MW), and thermal and mechanical properties, in addition to other relevant statistical values. The analysis revealed that the median PHA productivity observed in the fed-batch feeding strategy was 0.4 g L^{-1} h^{-1}, which is eight times higher than that obtained from batch feeding (0.05 g L^{-1} h^{-1}). Furthermore, 3-hydroxyoctanoate and -decanoate were the primary monomers incorporated into mcl-PHA. The investigation also determined the median glass transition temperature (−43°C) and melting temperature (47°C), which indicated that mcl-PHA is a flexible amorphous polymer at room temperature with a median MW of 104 kDa. However, information on the monomer composition or heterogeneity and the associated physical and mechanical data of mcl-PHAs is inadequate. Based on their mechanical

Abbreviations: 3HDD, 3-hydroxy dodecanoate; BMBF, Bundesministerium für Bildung und Forschung; BMEL, Bundesministerium für Ernährung und Landwirtschaft; DSP, downstream process; FFA, free fatty acids; lmw, low-molecular-weight; mcl-PHA, medium-chain-length polyhydroxy-alkanoate; PHA, polyhydroxyalkanoate; scl-lcl-PHA, short-chain-length-long-chain-length polyhydroxyalkanoate; scl-mcl-PHA, short-chain-length-medium-chain-length polyhydroxyalkanoate; SEM, Scanning electron microscopy.

values, the mcl-PHAs can be classified as semi-crystalline polymers (median crystallinity 23%) with rubber-like properties and a median elongation at break of 385%. However, due to the limited mechanical data available for mcl-PHAs with known monomer composition, identifying suitable processing tools and applications to develop mcl-PHAs further is challenging.

KEYWORDS
biopolymer, downstream processing, medium-chain-length, polyhydroxyalkanoate, thermal and mechanical properties

1 | INTRODUCTION

Due to the necessity for more sustainable processes and materials, efforts are being made to substitute fossil-based polymers with those derived from renewable sources. Polymers obtained from plants or microbes fulfil this requirement and are also biodegradable. Polyhydroxyalkanoates (PHAs) are important biopolymers discovered in bacteria in 1926 by Lemoigne [1]. Under stress conditions in excess carbon, these biopolyesters accumulate as intracellular granules for carbon and energy storage [2]. Research on PHAs was initially started in the early 90s and has gained considerable momentum in the past 20 years, as indicated by the number of publications, patents, and articles (Figure 1).

PHA is a natural polymer consisting of different (R)-β-hydroxy fatty acids comprised of alkyl chains of variable length. PHAs are classified into three groups based on the number of carbon atoms in the monomer: short-, medium-, or long-chain length PHAs (scl, mcl, and lcl-PHAs, respectively). The scl-PHAs, consisting of 3–5 carbon atoms, are the most abundant and well-characterized PHA (e.g., poly-3-hydroxybutyrate and poly-3-hydroxyvalerate). mcl-PHAs, comprising 6–14 carbon atoms, are mainly produced by *Pseudomonas sp*. [3]. However, lcl-PHAs, consisting of over 14 carbon atoms, are rare and less studied [4, 5].

Apart from the classification based on carbon atoms, PHAs can also exist as homo- or copolymers (Figure 2). PHA copolymers, including poly-3-hydroxybutyrate-co-poly-3-hydroxyvalerate (P3HB3HV), are mainly produced by *Cupriavidus necator* (formerly known as *Ralstonia eutropha*) or *Azohydromonas lata* (former known as *Alcaligenes latus*) through constant feeding of structurally related precursor molecules. PHA copolymers contain more than two either scl and mcl/lcl monomers or two mcl-PHAs monomers. These copolymers are arranged randomly or in block patterns. Since the first study showing the production of scl-lcl-PHAs from one microorganism, very few studies have investigated it further [7, 8].

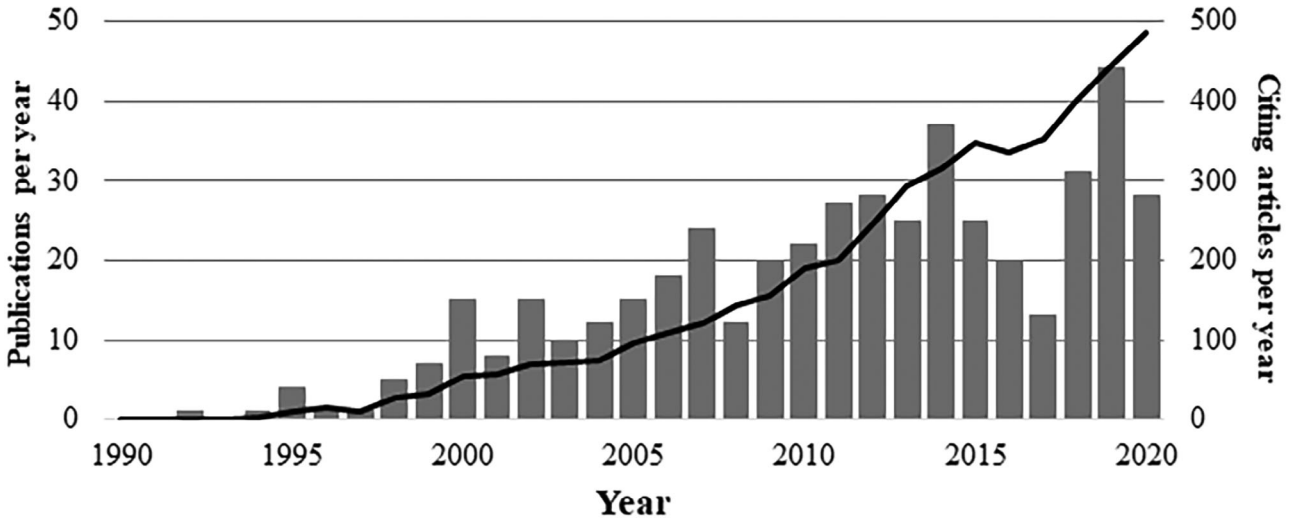

FIGURE 1 Overview of publications and citations per year from the WoS databases (©Clarivate 2023). Search terminology "medium-chain-length" and "polyhydroxyalkanoate*" in 1990–2022. The bar graph represents publications per year, and the line represents the number of citations on these articles.

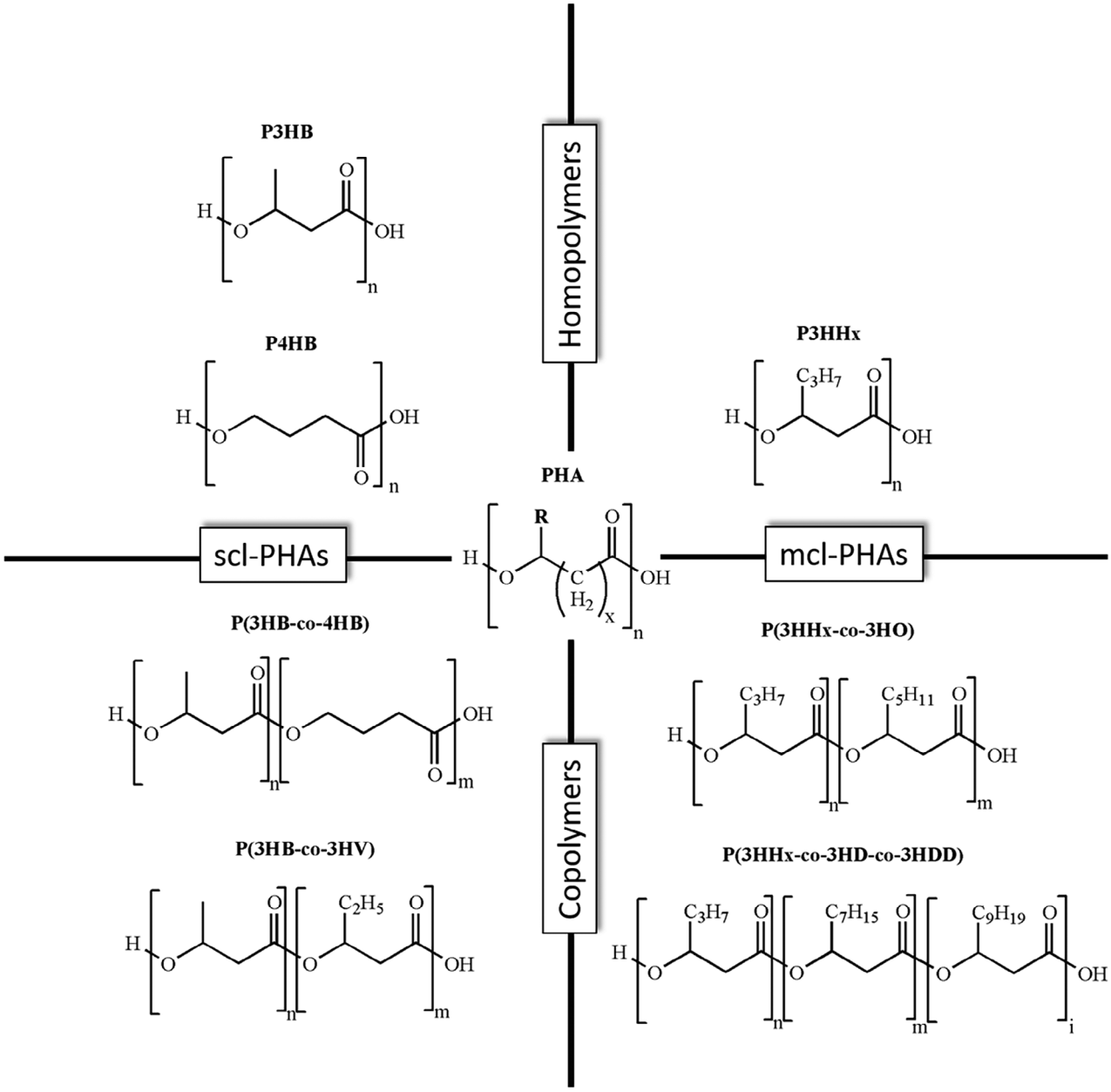

FIGURE 2 Classification of PHAs based on the chain length and diversity of the monomers, mcl = medium-chain-length, scl = short chain length (adapted from [6]).

Recent reviews published by several authors have focused on the biosynthetic pathways from the feed to the mcl-PHA production using genetically engineered microorganisms, fermentation strategies, downstream processing, properties, and applications, highlighting various feedstock and companies producing mcl-PHA globally [9, 10].

This review focuses on the wild-type strains, different substrates, and feeding strategies applied to achieve high mcl-PHA concentrations, providing an extensive and factual summary of the different approaches. Further, we discuss various analytical tools and methods available for qualitative and quantitative analysis of mcl-PHA, which are rarely reviewed. We have also systematically listed and evaluated the characteristics and properties of mcl-PHA to identify technical values and provided comparable statistical data representing the average mcl-PHA properties.

2 | DATA COLLECTION AND PROCESSING

For collecting data, we used the "Web of Science" (WoS) database to perform a literature search using keywords such as "medium-chain-length," "ferment*," and

"polyhydroxyalkanoate*," excluding hits with "genet*." Out of 141 articles, we included 90 articles in our literature review encompassing topics such as fermentation development or characterization, not compounding, blending, or application of commercial PHAs. Furthermore, studies dealing with mixed microbial consortia and/or genetically engineered bacteria were excluded. The papers were analyzed, ordered, and summarized to calculate values representative of most mcl-PHA properties. As the downstream processing of the mcl-PHA is similar to that of the scl-PHAs, it covers only a small part of this review.

Medians have been calculated across all collected data. The data concerning the fermentative PHA production have been split into related (fats and fatty acids) and unrelated (sugars, sugar alcohols, and volatile fatty acids) for growth behavior.

3 | mcl-PHA PRODUCTION

This section covers several factors affecting the production of mcl-PHA and its monomer composition, such as choice of microorganism, substrate, feeding strategy, fermentation parameters, and nutrients.

3.1 | mcl-PHA-producing microorganisms

In 1983, mcl-PHA granules were first detected when *Pseudomonas oleovorans* GPo1 was grown in 50% (v/v) n-octane [11]. Since then, several wild-type bacteria, mostly Gram-negative, that accumulate mcl-PHA have been identified. Nonetheless, the association between Gram-negative/Gram-positive and their ability to accumulate mcl-PHA is unclear. Most bacteria producing mcl-PHA were fermented under aerobic conditions and nutritional stress, especially nitrogen [12] and phosphorus limitation [13, 14], and, in some cases, under limited oxygen conditions [15].

Apart from *Pseudomonas* species, several other microorganisms, such as *Streptomyces* sp. JM3 (Gram-positive) [16] and *Enterobacter* FAK 1384 (Gram-negative) have been identified and investigated as mcl-PHA producers [17]. However, *Pseudomonas*, a rod-shaped, Gram-negative soil bacterium, remains the most studied one. Among them, *P. putida* (formerly known as *P. oleovorans*), *P. chlororaphis, P. resinovorans*, and *P. citronellolis* are well known for mcl-PHA production and can grow on diverse feedstocks, including carbohydrates, fatty acids, and alcohols.

Our data analysis showed that the highest reported biomass concentration was achieved with *P. putida* KT2440 (160 g L^{-1}) using waste cooking oil as a substrate. A significant amount of PHA (74% of the cell dry weight) was obtained when these bacteria were fed with a mixture of decanoic acid, acetic acid, and glucose [18, 19], indicating that *P. putida* performs high cell density fermentation, providing, at least theoretically, a high number of PHA producers per volume. Moreover, the utilization of the waste substrate for this process also has a positive economic impact.

Although *Pseudomonas* sp. is the most widely used mcl-PHA producer, the final biomass concentration and mcl-PHA accumulation have been shown to vary significantly based on the process conditions and the type of carbon sources used. Most mcl-PHAs are produced at ambient growth temperatures between 28°C and 30°C. Meanwhile, mcl-PHA production has also been reported in certain thermophilic bacteria, such as *Bacillus thermoamylovorans* PHA005, that can accumulate 63% of cell dry weight (CDW) mcl-PHA when grown on octanoate at 45°C [20]. Satoh et al. [21] cultured another thermotolerant species of *Pseudomonas* (SG4502) on biodiesel by-products, which can potentially accumulate 40% mcl-PHA consisting of even-numbered C4–C12 monomer units at 45°C. Using these thermophilic organisms could be advantageous for producing mcl-PHA on an industrial scale, as the sterility of the bioreactor increases when it is operated at higher temperatures [20, 21].

3.2 | Substrates for mcl-PHA production

For mcl-PHA production, the carbon sources influence the cell growth rate, PHA titer, and the proportion and type of monomers in the polymer [50, 53]. These substrates can be classified into two groups (Figure 3). The first group consists of substrates structurally related to mcl-PHA monomeric structure, including fatty acids and oils, which can be metabolized via the β-oxidation pathway [24]. The chain length of the substrate is reflected in the monomer composition. As the fatty acids in the substrate are truncated by one acetyl-CoA at each β-oxidation cycle, the monomeric spectrum mainly consists of the fed fatty acids and their shortened form. The extent of shortening is dependent on the number of fatty acids passing through the β-oxidation cycles [54].

The second group contains carbon sources structurally unrelated to the mcl-PHA monomers, such as sugars, volatile fatty acids, and glycerol [55, 56]. Carbohydrates are converted into acetyl-CoA through glycolysis and then into mcl-PHA through the de novo fatty acid biosynthesis pathway [52, 57]. This requires the temporary fixation of CO_2 onto acetyl-CoA to form malonyl-CoA, commonly recognized as the rate-limiting step in the metabolic pathway.

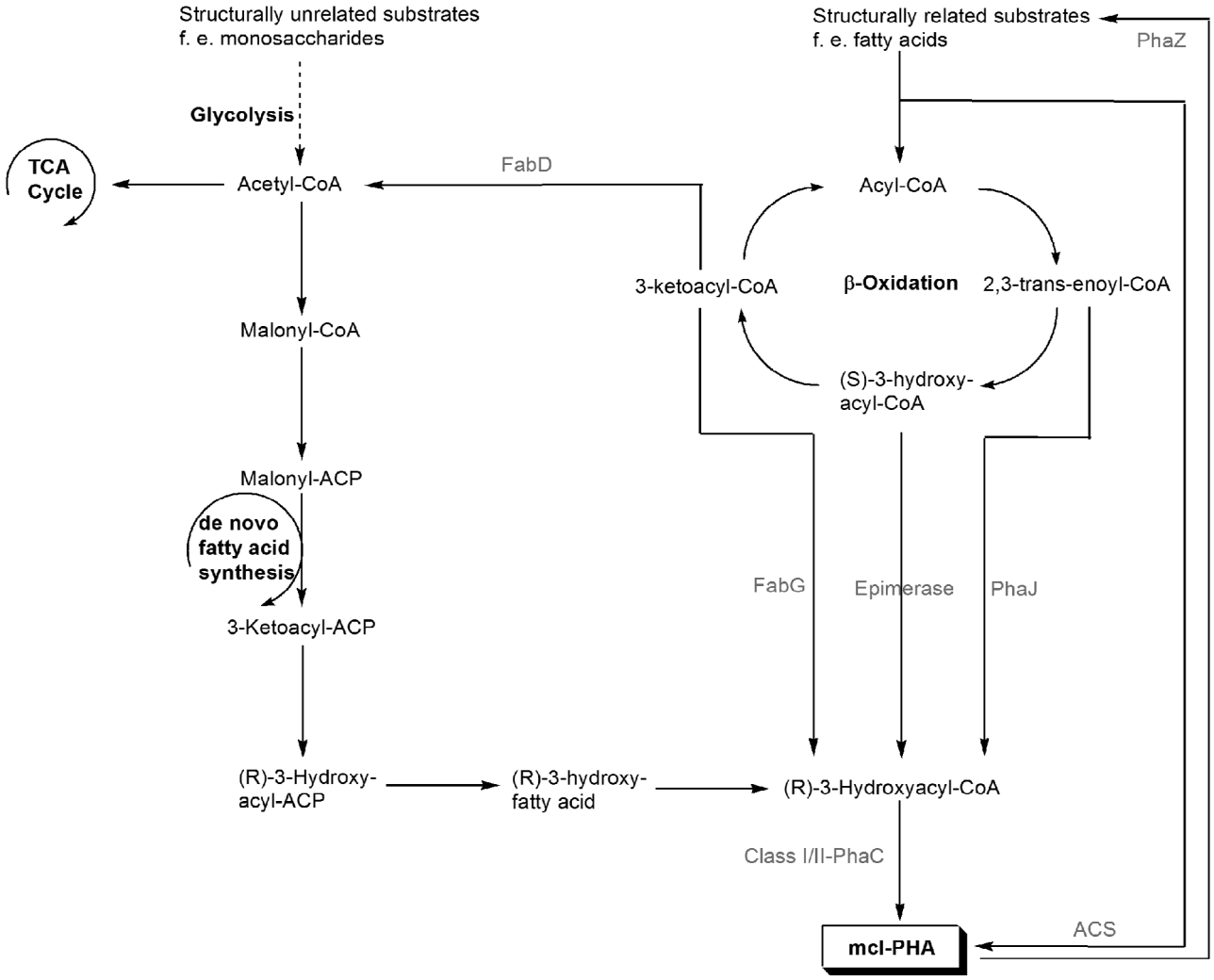

FIGURE 3 Metabolic processing of structurally related or unrelated substrates to mcl-PHA (adapted from [9, 10]). ACP, acyl carrier protein; ACS, acyl CoA-synthase.

We collected and analyzed data to determine the median values of biomass growth, PHA productivity, and yield on both substrate types. The analysis showed a higher median specific growth rate (0.46 h^{-1}) on structurally unrelated carbon sources than related carbon sources (0.22 h^{-1}), mainly due to the presence of sugars. While PHA production was more efficient on related carbon sources, with a median productivity of 0.36 g L^{-1} h^{-1} and a median PHA yield of 52%, the productivity and yield were 6 and 3.5 times less than unrelated carbon sources. This supports the commonly used process of growing biomass on sugars and changing the feed to fatty acids during the production phase (Section 3.3). Moreover, most studies have used structurally related substrates as significant carbon sources for producing mcl-PHA (Table 1).

A study demonstrated that even-numbered C8 and C10 chains were incorporated into mcl-PHA when *P. mendocina* 0806 was grown on citrate and glucose. When oleic and myristic acids were used as C sources, a C12-mcl-PHA constituent was also formed [67]. Follonier et al. [25] illustrated that the distribution of mcl-PHA monomers is comparable when unrelated C sources were used because acetyl-CoA is the primary precursor in the de novo pathway, whereas in β-oxidation metabolism, the fatty acids are the precursors. Therefore, the longer the fatty acid chain, the higher the proportion of long-chain monomers in the mcl-PHA polymer. Consequently, the tailored monomer composition with specific properties can be adjusted by selecting the feedstocks [25, 49]. For example, in the study with *P. putida* KTQQ20, it was shown that when the hexanoic acid proportion increased from 1 to 6 g L^{-1}, the 3-hydroxyhexanoate (3HHx) fraction increased from 16% to 63% [49]. Another investigation also indicated that feeding with octanoic acid increased the proportion of C8 monomers in the final polymer structure [15, 58].

Efforts have been made to find convenient substrate mixtures to maximize biomass growth and PHA production. Generally, a mixture of substrates, including fatty

TABLE 1 Overview of the achieved biomass concentration and mcl-PHA accumulation, yield, and productivity in the function of wild-type microorganisms and substrates. Only selected studies are shown. The data provided relate to the best results obtained within the studies.

Microorganism	Substrate	Fermentation strategy (vessel volume)	Biomass (g L^{-1})	PHA (% CDW)	PHA yield (g g^{-1})	PHA productivity (g L^{-1} h^{-1})	Cit.
P. putida KT2440	Waste cooking oil	Pulsed-fed batch (5 L)	160	36	0.28	1.93	[18]
	Decanoic acid, glucose, and acetic acid	Fed-batch (5 L)	75	74	0.86	1.16	[19]
	Glucose and nonanoic acid	Fed-batch (5 L)	71	56	0.66	1.44	[22]
	Nonanoic acid and 10-undecenoic acid	Fed-batch (5 L)	55	55	0.50	–	[23]
	Glycerol, octanoate	Batch (5 L)	26	34	0.21 (glycerol) 0.69 (octanoate)	0.18	[24]
	Pomace of white wine grapes, octanoic acid, and 10-undecenoic acid	Two phases: batch and fed-batch (300 L)	14	41	0.79	0.10	[25]
	Waste frying oil	Batch (3 L)	3	30	0.45	0.01	[26]
P. putida KT2442	Oleic acid, linoleic acid, and other fatty acids	Two-phase Fed-batch (20 L)	126	54	0.70	–	[27]
	Corn oil hydrolysate	Fed-batch (5 L)	109	28	–	0.68	[28]
	Octanoic acid	Fed-batch (7 L)	42	65	0.54	0.83	[29]
P. putida IPT046	Glucose and fructose 1:1	Fed-batch (8 L)	50	63	0.19	0.80	[14]
P. oleovorans	Octane	Fed-batch (3 L)	112	8–28	–	0.34	[30]
	n-octane in both reactors	Two-stage chemostat (3 L reactors)	18	63	–	1.06	[31]
	Octanoic acid	Fed-batch (5 L)	17	38	0.22	0.07	[32]
P. putida CA-3	Butyric acid and decanoate	Fed-batch (5 L)	90	65	0.52	1.63	[33]
P. chlororaphis	Waste cooking oil	Pulsed-fed batch (5 L)	82	21	0.08	0.36	[13]
	Biodiesel from waste animal fat	Fed-batch (5 L)	42	15	–	0.14	[34]
P. putida GPo1	Sodium octanoate and octanoic acid	Fed-batch (650 L)	53	60	0.41	0.76	[35]
P. citronellolis DSM 50332	Saturated biodiesel fraction	Pulsed-fed batch (5 L)	42	27	–	0.05	[36]
P. putida LS46	Octanoic acid	Pulsed-fed batch (7 L)	29	61	0.52	0.66	[15]
		Batch (7 L)	2	57	0.62	0.08	[37]
P. putida GO16	PET pyrolysis product and waste glycerol	Fed-batch (19.5 L)	19	33	–	0.13	[38]
P. putida Bet001	Palm kernel oil	Batch (0.25 L)	17	35	0.64	0.76	[39]
	Heptanoic and oleic acid	Batch (shake flask)	5.4	36	–	–	[40]
P. resinovorans	Olive oil deodorizer distillate	Fed-batch (10 L)	13	36	0.21	0.25	[41]
	Apricot pomace hydrolysate	Batch (3.7 L)	10	12	–	0.03	[42]
	Apple pomace	Fed-batch (1 L)	4	25	0.4	–	[43]

(Continues)

TABLE 1 (Continued)

Microorganism	Substrate	Fermentation strategy (vessel volume)	Biomass (g L^{-1})	PHA (% CDW)	PHA yield (g g^{-1})	PHA productivity (g L^{-1} h^{-1})	Cit.
P. putida sp.	Glucose	Batch (3 L)	9	3.0	0.01	–	[44]
Pseudomonas sp. PAMC 28620	Glycerol	Batch (1 L)	8	52	–	0.03	[45]
C. necator TISTR 1095	Tuna condensate	Three cycles repeated batch (5 L)	7.5	50	–	0.06	[46]
Pseudomonas sp. Gl01	Rapeseed oil	Pulsed-fed batch (7.5 L)	7	44	–	0.04	[47]
	Waste palm oil	Fed-batch (7.5 L)	5	43	–	0.06	[48]
P. putida KTQQQ20	Glucose, hexanoic, and dodecanoic acid	Batch (0.5 L)	5.1	35	–	–	[49]
	10-undecenoic acid	Two-stage chemostat (2.5 L)	1.2	25	0.72 (mol mol^{-1})	–	[50]
B. thermoamylovorans PHA005	Sodium octanoate	Batch (3 L)	2.7	63	0.68	0.05	[20]
Pseudomonas sp. SG4502	Biodiesel fuel by-product	Batch (3 L)	1.5	40	–	–	[21]
P. mosselii TO7	Glycerol	Batch (0.25 L)	1.3	48	–	0.01	[51]
P. putida S12	Sludge palm oil	Batch (shake flask)	1	41	–	–	[52]

- Data not available.

acids with different carbon chain lengths (saturated or unsaturated), is commonly used for mcl-PHA production (Tables 1 and 2). Co-feeding glucose and fructose to *P. putida* IPT 046 resulted in a biomass concentration of 50 g L^{-1} containing 63% mcl-PHA [14]. Other substrate combinations, including fatty acids, waste materials, and simple sugars, are frequently used to improve PHA production. For example, when glucose was employed as a co-substrate with nonanoic acid to feed *P. putida* KT2440, the PHA yield was 25% higher than when nonanoic acid was used as the sole carbon source [22]. This also resulted in *P. putida* KT2440 growth up to a concentration of 71 g L^{-1} with 56% mcl-PHA content, demonstrating that co-feeding carbon sources increases the yield and enables utilization of inexpensive or waste material as substrates.

3.2.1 | Crude glycerol

Due to the easy availability and sustainability of raw glycerol, the by-product of biodiesel manufacturing represents a feasible carbon source for mcl-PHA production [38, 57]. Additionally, using glycerol as a substrate reduced the cost of mcl-PHA bioproduction compared to pure alkanes or related fatty acids [45]. mcl-PHA accumulation was shown to be increased from 1.3% to 42% of CDW under the co-metabolism of glycerol and octanoate when fed to *P. putida* [19, 24]. Therefore, glycerol, as an unrelated carbon source, was shown to promote cell growth and propagation, whereas octanoate, as a structurally related carbon source, enhances mcl-PHA accumulation in *P. putida* KT2440. This is supported by the fact that the polymer composition was similar when grown solely on octanoate.

3.2.2 | Long-chain fatty acids

Long-chain fatty acids (LCFAs) are the most studied substrate for mcl-PHA production (Table 1) because of their structural similarity to mcl-PHA monomers. Several species of *Pseudomonas*, such as *P. chlororaphis*, *P. putida* KT2440, and *P. resinovorans*, metabolize LCFAs into mcl-PHA via β-oxidation [18, 59]. Studies have shown that LCFAs are a suitable carbon source for mcl-PHA production and high cell density fermentation. For example, in a high-cell density approach using corn oil hydrolysate as substrate, *P. putida* KT2442 reached a cell concentration of 109 g L^{-1} with 28% mcl-PHA accumulation [28]. Similarly, another study reported 126 g L^{-1} of biomass

TABLE 2 Overview of the molecular weight and thermal characteristics of mcl-PHAs as the function of microorganisms, substrates, and composition. Only selected studies are shown as those that did not state the exact values for PHA composition or did not provide thermal and molecular weight characteristics were excluded. PHAs consisting of monomers with odd carbon atoms and unsaturated monomers are discussed in the text. *Unsaturated monomers are not shown; the percentage share is added to the respective saturated monomers with the same chain length.

Microorganism	Substrate	3HHx	3HO	3HD	3HDD	3HTD	3HHD	M_w (kDa)	PDI	T_g (°C)	T_m (°C)	Cit.
B. thermoamylovorans PHA005	Sodium octanoate	–	24	15	–	13	39	–	–	1.3	68	[20]
P. chlororaphis 555	Waste cooking oil	7	36	37	20	–	–	18	1.9	−64	–	[13]
P. fulva TY16	Decanoic acid	7	49	44	–	–	–	43	1.1	−39	48	[84]
	Octanoic acid	10	79	11	–	–	–	43	1.1	−35	56	
	Toluene	4	27	55	14*	–	–	43	1.1	−42	50	
P. mendocina CH50	Coconut oil	–	30	48	21	–	–	333	2.4	−42	48	[61]
P. mosselii TO7	Crude glycerol	1	71	25	4	–	–	97	1.3	–	49	[51]
P. oleovorans	Octanoic acid	8	92	–	–	–	–	396	1.8	−33	61	[32]
P. putida Bet001	Octanoic acid	3	46	39	12	–	–	65	2.1	−46	–	[40]
P. putida GO16	Terephthalic acid and waste glycerol	2	22	46	28*	2*	–	70	1,89	−52	45	[38]
P. putida KT 2440	Cider by-products	3	23	61	12*	–	–	47	2.2	−42	47	[43]
P. putida KTOY06	Decanoate	10	43	33	15	–	–	100	1,3	−44	53	[85]
P. putida sp. coculture	Aromate mixture	–	16	64	19*	–	–	87	3,8	−48	44	[86]
P. putida S12	Sludge Palm Oil	5	30	29	17	19*	–	106	2.4	−42	35	[52]
P. resinovorans NRRL B-2649	Olive oil deodorizer distillate	12	48	31	8	<1	–	30	1.5	−16	36	[41]
P. sp. GIo1	Saponified waste palm oil	–	45	40	15	–	–	96	2.3	−46	86	[48]
	Rapeseed oil	8	53	37	3	–	–	144	2.5	−38	–	[47]

- Not determined or data not available.

containing 54% CDW mcl-PHA using a mixture of pure LCFAs in a 20 L reactor [33]. mcl-PHA productivity using LCFA-containing complex substrates from renewable resources or waste streams was as high as that achieved with pure fatty acids or carbohydrates (Table 1). For instance, a higher PHA productivity of 1.93 g L^{-1} h^{-1} was achieved from waste cooking oil compared with 1.44 g L^{-1} h^{-1} using glucose and nonanoic acid (Table 1).

LCFAs have low solubility in aqueous media due to the high concentration of palmitic acid, which renders the substrate solid at room temperature [18]. This poses rheological and mass transfer challenges, which must be overcome by maintaining the liquid state of the hydrolysates at high temperatures and effectively introducing them into the cells. This, in turn, makes it challenging to homogenize samples for subsequent analytical procedures or mathematical modeling. Besides, the substrate concentration as an indicator of fed-batch strategies would not be accurate [13].

As substrate costs constitute the majority of the total production cost, substituting them with cheaper materials would be ideal. Therefore, fatty acid sources, including kernel oil, rapeseed oil, vegetable oil, waste palm oil, and waste cooking oil, could be potential substrates for economical carbon sources for mcl-PHA production studies [18, 39, 47, 48, 52].

3.2.3 | Waste-containing carbohydrates

Recent studies investigate waste-containing sugars, such as starch [56] and fruit pomaces [25, 43]. Follonier et al. [25] demonstrated that, in a 100 L two-phase fermentation, hydrolyzed pomace of white wine grapes could be used as a carbon source to produce PHA, completely replacing glucose and decreasing the substrate price and overall process costs [25]. However, utilization of these alternative feedstocks requires a preliminary pre-treatment step, such as

saponification [39], transesterification [34, 59], chemical or enzymatic hydrolysis [18], liquid extraction, filtration [25], dehydration, and pressing, which can be expensive and time-consuming. Moreover, due to the high variability of the complex matrices, characterizing specific raw material batches, especially in composition, is necessary. Therefore, establishing a growth and production medium that maintains the reproducibility of fermentation is crucial.

3.3 | Feeding strategies for mcl-PHA production

Traditionally, fermentation is performed in shake flasks or batch mode, essential to study and identify the growth kinetics of microorganisms, optimal growth parameters, and preferred nutrient composition. However, cell growth and PHA productivity are much lower in the batch mode than those achieved with other modes of operation (Table 1).

The highest cell density achieved using wild-type microorganisms in pulsed-fed-batch mode was 160 g L^{-1} [18] compared to 26 g L^{-1} for batch-type [24] and 112 g L^{-1} in fed-batch feeding strategies [30]. The maximum mcl-PHA productivity obtained using batch, chemostat, fed-batch, and pulsed-fed-batch strategies were 0.76 [24], 1.06 [30], 1.63 [33] and 1.93 g L^{-1} h^{-1} [18], respectively. Comparison of the median values of batch and fed-batch processes revealed no significant difference in the median PHA content (PHA_{batch} = 36%, $PHA_{fed\text{-}batch}$ = 38%) or yield (Y_{batch} = 0.45 g g^{-1}, $Y_{fed\text{-}batch}$ = 0.51 g g^{-1}). However, in the fed-batch process, the median PHA productivity (q_{batch} = 0.05 g L^{-1} h^{-1}, $q_{fed\text{-}batch}$ = 0.40 g L^{-1} h^{-1}) and biomass concentrations in CDW (CDW_{batch} = 4.3 g L^{-1}, $CDW_{fed\text{-}batch}$ = 42.2 g L^{-1}) were higher. These dynamic values show that the feeding strategy and bioreactor operation mode are essential for biomass growth and PHA productivity. Moreover, these feeding strategies overcome the disadvantages of substrate inhibition or nutrient limitation during batch process.

3.3.1 | Fed-batch and pulsed fed-batch strategies

Currently, fed-batch and pulsed-fed-batch cultures are considered the most productive for mcl-PHA synthesis. They also reduce the possibility of substrate inhibition or toxicity during fermentation. Fed-batch strategies have been reported for several *Pseudomonas* species. For instance, using an exponential feeding strategy, *P. putida* KT2440 accumulated mcl-PHA with a productivity of 1.16 g L^{-1} h^{-1}. Generally, the cell concentrations, mcl-PHA content, and productivity obtained using the pulse-fed batch mode are higher than those achieved using other methods. Using a pulse-fed batch, an mcl-PHA productivity of 1.93 g L^{-1} h^{-1} was achieved by supplying the substrate in 25 pulses over 30 h [18]. Similarly, using the same approach, 61% CDW mcl-PHA accumulation was seen in *P. putida* LS46 with a productivity of 0.66 g L^{-1} h^{-1} [15].

Measuring the substrate consumption rate in real time is challenging. Therefore, reliable pulse-fed batch processes are usually developed based on the growth stage, metabolism, and viability of the cell culture. CO_2 concentrations in the exhaust gas stream or O_2 concentration in the bioreactor are used as indicators to control the physiological cell state and substrate level in the medium indirectly [13, 15, 18]. For example, a drop in the CO_2 concentration or increased dissolved oxygen indicates decreased metabolic activity. A 25% drop in the CO_2 concentration is a trigger to start automatic feeding [19]. A similar concept is also adapted to develop pulse-fed batch feeding, where the substrate is fed intermittently using the dissolved oxygen (DO) concentration in the bioreactor.

The effect of adding different (micro)nutrients is poorly understood. Hence, we could not obtain any trends regarding the feeding time or the concentration of the added nutrients. Instead, these parameters depend on the microorganism and its growth kinetics. Thus, further research is required to study the effect of micronutrients on mcl-PHA production to increase the productivity and yield of PHA.

3.3.2 | Continuous processes

An industrial-scale mcl-PHA production process preferably requires a continuous process. Continuous mcl-PHA production has been shown using a two-stage chemostat for biomass growth and PHA accumulation. In the first reactor, biomass is allowed to grow to achieve high cell density, while the broth containing a high biomass concentration is transferred to the second reactor, which is operated under optimal conditions for PHA accumulation. In this study, n-octane was used as the carbon source to feed *P. oleovorans* ATCC 29347 with optimum dilution rates of 0.22 and 0.16 h^{-1} in the growth and accumulation reactors, respectively. Under these conditions, the biomass concentration and mcl-PHA productivity were 18 g L^{-1} (63% mcl-PHA) and 1.06 g L^{-1} h^{-1}, respectively [31]. Similarly, another study showed productivity of 1.2 g L^{-1} h^{-1} (25% mcl-PHA) using *P. putida* KTQQ20 [50]. In both studies, the culture volume of the first stage was continuously transferred to the second reactor, and a steady state was achieved after 24 h or more.

Very few studies have focused on developing continuous fermentation processes, as operating two reactors for biomass growth and PHA accumulation is cumbersome and expensive. Furthermore, a steady state does not guarantee that the biomass has achieved a maximum PHA accumulation capacity and entirely consumed the substrate supplied into the bioreactor. Therefore, a two-phase fermentation, described in the following section, might be ideal for producing mcl-PHA.

3.3.3 | Two-phase fermentation

The optimal conditions for cell growth and mcl-PHA accumulation differ. Nitrogen and phosphorus are essential to achieve high cell density during biomass growth. In contrast, nutrient limitation is the critical factor that triggers PHA production under excess carbon conditions during PHA accumulation. Therefore, two-phase fermentation systems have performed better than two-stage chemostat fermentation [31]. Moreover, the former requires a single reactor, whereas the latter needs two different reactors. Generally, the first phase aims to achieve high biomass concentration, whereas the PHA accumulation occurs in the second phase. While the second phase is usually initiated by nitrogen limitation [27, 34], different stress factors, including phosphorus [60] or oxygen limitation [37], have also been reported. Consequently, two-stage fermentation has been widely used in the studies included in this review [50, 61].

Various feeding strategies can be used with two-phase fermentation. For biomass growth, batch or fed-batch feeding can be utilized. For PHA accumulation, fed-batch, pulse, or continuous feeding could be implemented depending on the substrate type. Using a combination of batch growth stage and linear fed-batch polymer accumulation, a *P. putida* KT2440 concentration of 14 g L^{-1} with a 41% mcl-PHA content was obtained [25].

Although these feeding strategies have been extensively explored, they have not been widely replicated on a pilot or production scale. Thus, broad commercialization of mcl-PHA is yet to be achieved, which requires more pilot-scale research in large fermentation volumes to demonstrate the feasibility and productivity of mcl-PHA on an industrial scale.

4 | DOWNSTREAM PROCESSING

As downstream processing (DSP) is crucial for extracting mcl-PHAs from biomass, determining its properties without interfering with the effects of potential contaminants to exploit their full potential, is necessary. Furthermore, many applications require a high degree of purification. However, this review focuses on the production and properties of mcl-PHA rather than DSP. Moreover, the processes and methods currently used to purify mcl-PHAs do not differ significantly from those used for scl-PHAs. Thus, we have only provided a summary of the established methods used to purify mcl-PHA on a laboratory scale and then proceeded with a detailed analysis of the relevant polymer characteristics.

The most frequently used purification method is solvent extraction, consisting of three significant steps (Figure 4): Separation and drying of biomass, extraction, and precipitation. Furthermore, additional refining steps can be performed to increase the purity of the polymer.

After isolating the biomass from the culture broth by centrifugation or filtration, the harvested cells are either freeze-dried [61, 62] or oven-dried [40]. Several studies have shown that biomass should be pre-treated to weaken the cell membrane and promote cell lysis. To achieve this, dried biomass is degreased overnight using ethanol [34] or methanol [63] at room temperature or ethanol by reflux [64]. Then, the biomass is washed with saline solution and n-hexane to remove loosely bound non-PHA material [40] and excess fatty acids, respectively [32]. Moreover, heat pre-treatment by autoclaving the fermentation medium supported cell lysis and nucleic acid solubilization in enzymatic DSP processes [65]. Some studies used pre-treatment with NaOCl, a strong oxidizing agent, to disrupt cell membranes and enhance recovery [66].

This is followed by PHA extraction from the cells, usually done using organic solvent extraction via stirring or the well-known Soxhlet apparatus. In the Soxhlet apparatus, PHA is selectively transferred from a sample matrix into the solvent, and the solvent is regenerated by distillation through a periodic process. Jiang et al. [67] reported that Soxhlet extraction is more effective than direct extraction on a bench scale. However, this apparatus is not suitable for scaling up. The PHA recovery yield from solvent extraction depends on the type of solvent. Conventionally, halogenated solvents are widely used because they provide high polymer purity and recovery yield [9]. However, mcl-PHAs are also soluble in non-halogenated solvents, such as methyl tert-butyl ether, ethyl acetate, and acetone. Jiang et al. [67] achieved >86% recovery and 94% polymer purity using acetone to extract mcl-PHA from methanol-pretreated biomass.

After extraction, the cell debris is separated from the PHA-containing solvent through filtration [32, 40], centrifugation, or decantation. Then, the PHA is precipitated in ice-cold methanol or ethanol, followed by further separation and subsequent drying [34, 63].

Although solvent extraction is a significantly efficient method, it is disadvantageous from an economic and

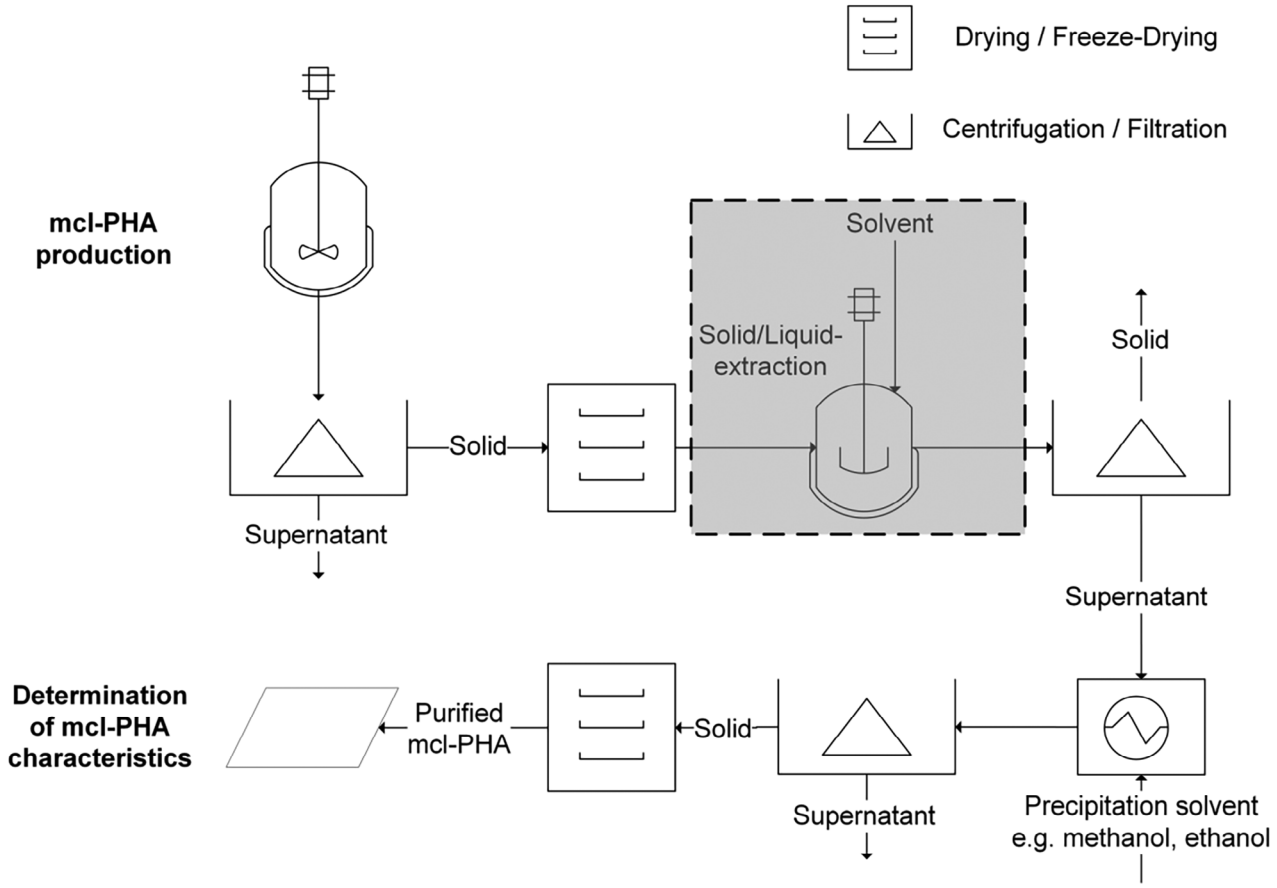

FIGURE 4 Flow scheme focusing on different unit operations of mcl-PHA downstream processing. The most relevant purification step, solvent extraction, is highlighted.

environmental point of view because a large volume of toxic solvents is required. Therefore, for mcl-PHA extraction, a comprehensive screening should be done to evaluate green and sustainable solvents, such as hydrophobic natural deep eutectic solvent (NADES), which exhibited a PHA recovery value and purity of 42% and 99%, respectively [68]. NADES comprises various naturally occurring or food-grade components mixed in specific proportions to create a eutectic mixture with unique solvent properties. However, the NADES formulation needs to be further optimized to improve the recovery rate of the solvent.

Other solvent-free extraction methods have also tested and studied for mcl-PHA purification. These methodologies are based on dissolving and digesting the nonpolymeric cell material to recover mcl-PHA. Yasotha et al. [65] achieved a recovery yield of 90% using a two-step digestion method. Purification consisted of wet biomass digestion using Alcalase® and SDS in the first step, followed by a second step with EDTA and lysozyme. Furthermore, the MW of PHA recovered by enzymatic treatment was higher than that of PHA extracted using chloroform [65, 69]. Apart from enzymatic digestion, methods such as acid, alkali, oxidant, and surfactant hydrolysis have also been implemented for the purification of PHA. Depending on these methods, the recovery rate varies between 75% and 95% [70]. The main disadvantage of acid and alkali hydrolysis is that the PHA polymer with lower MW is recovered [71]. Therefore, it is essential to select a suitable extraction method depending on the further application of PHA.

Few DSP methodologies have been described in detail and reported for pilot-scale extraction. Most authors conducted extraction and purification, with the only objective being subsequent polymer characterization, such as monomer composition, MW, molecular mass distribution, and its thermal and mechanical properties, to determine the suitable applications of the PHA [22, 34]. mcl-PHA characteristics and commonly used techniques for their determination are described in the following sections.

5 | mcl-PHA CHARACTERISTICS

The structural, thermal, and mechanical properties of mcl-PHAs, such as the MW and melting temperature,

determine their processability and application, and hence, should be frequently analyzed. This section examined the median values for different analytical methods based on relevant studies. These values were compared with those obtained from scl-PHAs and discussed, considering other relevant features, such as the purity or monomer composition of the mcl-PHAs.

5.1 | Chromatographic determination of the purity and monomer composition

Gas chromatography (GC) is the most frequently used technique to analyze mcl-PHA. It is an accurate and cost-effective method to analyze the monomeric composition [72] and to determine the purity of PHAs [65, 73], especially for scl-PHAs. However, analyzing the composition and purity of mcl-PHAs using GC is more challenging. For analysis, methanol transesterification under acidic conditions cleaves the polymer into its monomers and converts them into methyl esters. Furrer et al. [74] reported that GC might not be a reliable method for mcl-PHA due to the slow reaction kinetics of the transesterification of mcl-PHAs. However, this could be avoided by extending the incubation time.

Conventional detectors, such as flame ionization detectors, require standard methyl esters for calibration, which can be challenging because only a few are commercially available. In the case of a mass spectrometry (MS) detector, mass spectra can be identified with the help of online library databases (e.g., NIST). Irrespective of the detector used, differentiation between structural isomers is challenging using GC alone without MS coupling. Nevertheless, it remains the most prominent tool for analyzing mcl-PHA, as it is the only accurate method available to determine the degree of purification. Muhr et al. [36] validated the accuracy of GC in determining the chemical composition of mcl-PHA.

5.2 | Spectroscopic investigation

The main spectroscopic methods used to characterize mcl-PHAs are nuclear magnetic resonance (NMR) and Fourier-transformation infrared (IR) spectroscopy. The latter was the most widely applied qualitative method to investigate biopolymers in the reviewed publications.

5.2.1 | IR spectroscopy

Most studies used IR spectroscopy to confirm the excitation of mcl-PHA-specific vibrations, resulting in characteristic peaks, which can be utilized to identify mcl-PHAs and all PHAs in general [17]. A strong peak in the range of 1720–1740 cm^{-1} derived from an ester-specific vibration was identified and applied as a marker peak to confirm the presence of PHAs [20, 43, 45, 51]. The peaks at 2800−3000 cm^{-1} were assigned to methyl- and methylene-specific vibrations [40]. The band at this wavelength is more robust and splits into several peaks for mcl-PHAs because of the increased number of methylene groups and higher diversity of the chain lengths. Strong peaks at 1276 and 1130 cm^{-1} can be attributed to the asymmetric C O C and C O stretching [20].

Although IR spectroscopy offers excellent potential, only a few studies have exploited the obtained IR spectra for advanced investigations. For instance, Sathiyanarayanan et al. [45] determined the crystallinity index by a quotient of absorbances exploiting the bands at 1181 cm^{-1} (crystallinity-sensitive) and 1719 cm^{-1} (crystallinity-insensitive). Further, using a non-destructive IR-based method, PHAs accumulated within the bacterial cells were identified quickly, unlike using extracted PHAs [75].

However, as IR spectroscopy mainly identifies specific functional groups, not molecules, mcl-PHAs, and scl-PHAs can be differentiated qualitatively. Using IR to quantitatively differentiate between different PHAs in a mixture (to obtain a ratio of PHAs) is challenging due to similarities in the spectra. Thus, IR is mainly used to validate the presence of PHAs rather than provide information about the polymer's composition. It is, therefore, of limited value without applying advanced evaluation techniques or software.

5.2.2 | Nuclear magnetic resonance (NMR) spectroscopy

NMR spectra can provide more information and higher resolution than IR spectra. Commonly performed measurements, such as ^{1}H- and ^{13}C-NMR, have been applied to determine the monomer composition of the mcl-PHAs and their relative amounts. For example, a typical monomer composition of an mcl-PHA, from 3HHx to 3HDD, can be derived from Figure 5 with a numbered assignment of the C- and H-atoms. Figure 6 shows the representative ^{1}H- (a) and ^{13}C-NMR spectra (b) of mcl-PHA, predominantly composed of the monomer 3HD.

Considering ^{1}H-NMR, multiple peaks around 2.5 ppm can be assigned to α-carbon protons (methylene, see C-2 in Figures 5 and 6A,B), a peak downfield at 5.2 ppm can be assigned to the β-carbon (methine, C-3) proton. These are so-called *marker peaks* for PHAs in general [61]. The peak upfield around 1.5 ppm could be assigned to the

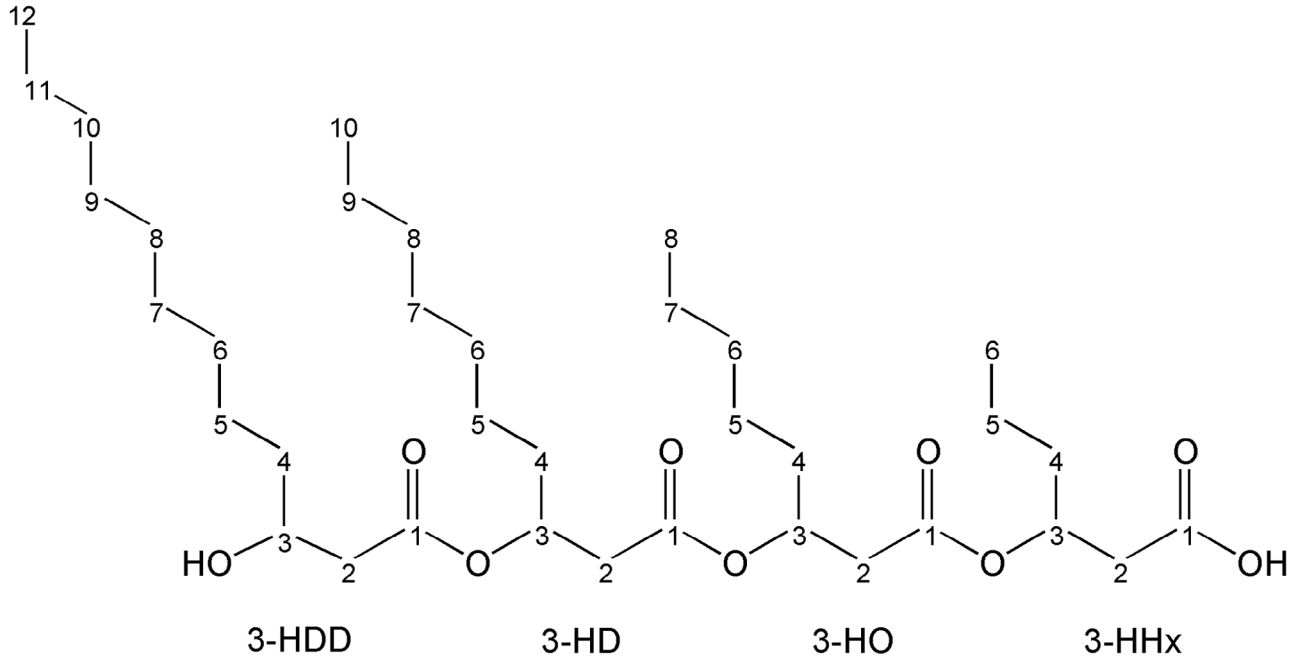

FIGURE 5 mcl-PHA structure and diversity of its monomers.

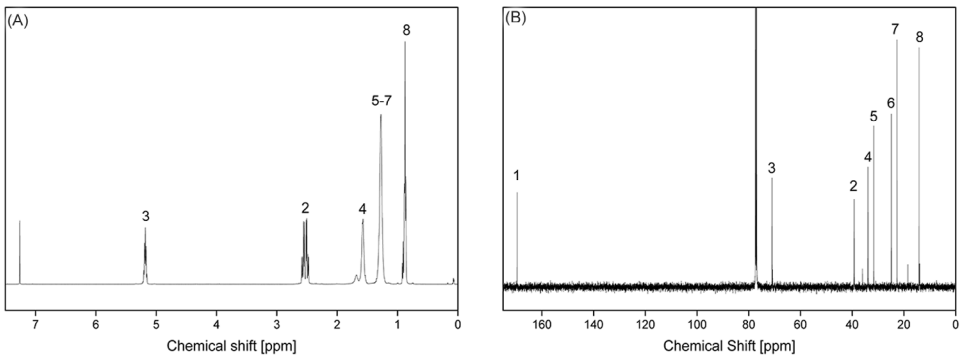

FIGURE 6 ^{1}H- (A) and ^{13}C-NMR spectra (B) of mcl-PHA mainly comprise 3HD. The numbers in the spectra assign the specific peaks of the C atoms themselves or the protons linked to them with the structure shown in Figure 5.

methylene protons of the γ-carbon (C-4). Peaks with a chemical shift below 1.5 ppm can be allocated to protons of the side-chain methylene groups (C5-7 in Figure 6A) [40]. Peaks at 0.8–0.9 ppm can be assigned to terminal methyl groups (C-8 in Figure 6A) [45]. The distinction of methylene hydrogen atoms in pendant alkyl chains by ^{1}H-NMR is complicated because of the commonly limited maximum field strength of the NMR spectrometers, thus moderate resolution and overlap of peaks. Double bonds in the side chains can be distinguished by additional peaks at approximately 2.0, 2.3, and 5.3 ppm [76].

^{13}C-NMR is another valuable method for obtaining the mcl-PHA's composition. A major peak can be identified at approximately 170 ppm from the carbonyl C-atom of the polymer backbone (C-1). α-, β-, and γ-carbon atoms can be identified at approximately 40 (C-2), 71 (C-3), and 35 ppm (C-4), respectively [45]. Olefinic C atoms have a chemical shift of 120–140 ppm [43]. For ^{1}H-NMR, the terminal methyl carbons resonate at a high field strength (C-8. upfield, 13–15 ppm) [43].

Unlike ^{1}H-NMR spectroscopy, ^{13}C-NMR is suitable only in exceptional cases or with time-consuming measurements to determine the relative distribution of the monomers in mcl-PHA. However, ^{13}C-NMR can be used to distinguish the peaks clearly, enabling the assignment of the respective carbon atom. Using an NMR spectrometer with strong magnetic fields, assigning the peaks to the respective building blocks is feasible even in mcl-PHA containing diverse monomers and several long-chain residues. For example, Muhr et al. [36] easily distinguished between 3-hydroxyoctanoate (3HO) and 3-hydroxydecanoate (3HD) and identified these as primary monomers based on the

peaks at 15 and 38 ppm. Further, 3HV and unsaturated building blocks were detected even in small amounts due to the high sensitivity of the NMR technique.

Shang et al. [28] used ^{13}C-NMR spectroscopy to confirm the effect of fatty acid composition and substrate concentration on the final monomer composition. They compared the NMR spectra *fingerprints* measured with mcl-PHA formed by *P. putida* KT2442 grown on pure oleic and linoleic acid with corn oil hydrolysate. Using ^{13}C-NMR, they confirmed that the incorporation of 3HDD and 3HωTD into mcl-PHA by *P. putida* grown on corn oil hydrolysate is due to the presence of oleic acid. The integration of 3HωDD and 3HTD anon results from linoleic acid, another major fatty acid in the corn oil substrate, suggesting that the composition of mcl-PHA could be target-oriented and adjusted by the choice of substrate.

Several reports have applied NMR to confirm that the produced polymer is or, at least, incorporates mcl-PHA [51] or to allocate the shifts to the different monomers in the mcl-PHA [77]. Although this also has an informational value, a solely qualitative analysis could be performed by other less cost- and time-intensive measurement methods, such as IR spectroscopy.

The values representing the chain length and the number of unsaturated monomers have been shown to be in good agreement with the NMR and GC-MS measurements. Although this enables experienced technicians/researchers to understand the monomer composition with NMR considering, for example, a highly diverse mcl-PHA or one with monomers of increased chain length, it offers the benefit of even locating the double bonds of unsaturated chains [78] or detecting structural isomers [79].

Furthermore, NMR can also determine and quantify lipid contaminants [70]. Linton et al. [80] showed that NMR could also be applied to determine the content and purity of PHA in a complex matrix. These NMR techniques must be further developed to routinely assess the degree of purification. However, NMR requires cost-intensive equipment and trained staff, whereas the GC or LC equipment needed to determine the purity and composition does not require high investment and skilled personnel.

5.3 | Determining the molecular weight using gel permeation chromatography

The MW of mcl-PHA, an essential characteristic, can be measured via gel permeation chromatography (GPC). Few studies have also used viscosimeter-based MW measurements, resulting in the viscosity-average molecular weight (M_V) [81, 82].

The MW of P3HB greatly determines its film-casting ability, thermal and processing behavior, and brittleness [83]. The same can be assumed for mcl-PHAs. Table 2 lists the Number-average molecular weight (M_n), weight-average molecular weight (M_w), and resulting polydispersity index (PDI) of various mcl-PHAs.

As MW distribution is commonly unimodal, one defined peak resulting from the chromatographic separation [36] can be evaluated. Analysis revealed a range of 11−396 kDa for M_w and a range of 6 to 216 kDa for M_n. The calculation of the medians investigated for all studies yielded a value of 104 kDa for M_w and 49 kDa for M_n. This is significantly lower than the median values commonly published for scl-PHAs (>250 kDa). High-molecular-weight (HMW) PHAs are generally desired because they show improved mechanical strength compared with lower MW analogs [87]. However, low-molecular-weight (LMW) mcl-PHAs, thus, have potential applications in the biomedical field, such as adhesive materials [43].

According to Zinn et al. [88], the MW of PHAs depends on the bacterial strain, polymerase copy number and expression level, growth conditions, and carbon source. This could only be partially confirmed in the case of the carbon source. Davis et al. [62] indicated that the M_W of *P. fluorescens* 555 mcl-PHA is slightly higher when grown on a grass hydrolysate than on a synthetic sugar mix. Other authors observed that applying a mixture of heptanoic and oleic acid does not significantly influence the MW compared to using oleic acid alone [40]. Similar results were seen during mcl-PHA production with *P. chlororaphis* 555 using rape seed oil and its hydrolysis product, as the M_w and M_n do not significantly differ [89].

Expectedly, the MW significantly depends on whether the carbon source is related, unrelated, or non-natural. Even when substrates within the same compound class are used, the MW difference can be significant due to the different metabolic pathways involved in degradation, as shown by Hanik et al. [50]. They observed a significant difference in the MW using a non-natural carbon source and a related substrate: 3-hydroxy-5-phenylvalerate and decanoate. M_n is approximately doubled using decanoate as the substrate.

Some substrates, such as glycerol, have a chain-terminating effect in the non-metabolized native form, which lowers the MW of mcl-PHA [21, 51]. Thus, a substrate with a unique composition commonly results in a higher MW than the mcl-PHAs achieved using heterogeneous substrates, such as waste cooking oil, because they are highly likely to contain chain-terminating compounds [18].

The extraction methods also affect the MW of mcl-PHA [90], specifically the solvent used for extraction. Bartels et al. [90] confirmed that, in addition to the monomer

ratio, the M_w of a P(3HB-co-3HHx) varies in the range of 134–199 kDa depending on the solvent used for extraction. This might be because the diffusion kinetics might differ for LMW and HMW mcl-PHAs in the respective solvents. A previous study suggested that the differences in removal efficiencies of polymeric impurities with charcoal might alter the MW and polydispersity indices (PDIs) [66, 91].

PDI represents the heterogeneity of the polymer's MW and is, in the case of mcl-PHAs, a function of cultivation conditions, the polymer recovery process, and the type of PHA synthase of the microorganism [84]. It has a substantial effect on the mechanical and processing properties. Highly polydisperse samples behave like a blend of LMW and HMW polymers: LMW polymers within the mixture could act as softeners and plasticizers, whereas HMW polymers contribute significantly to the melting viscosity. Although a high polydispersity is not necessarily disadvantageous, however, a low dispersity and a monodisperse polymer is more desirable. Most mcl-PHAs have a median PDI of 1.97. PDIs close to 1 are considered to represent nearly uniform and monodisperse polymer chains [84], as is the case for proteins or DNA. Higher PDIs were measured using synthetic compounds as substrates, such as 5-phenylvalerate [50] or aromatics [86].

Although MW values of mcl-PHAs have often been compared with previously published values, only few studies have determined the main factors influencing the MW of mcl-PHAs. According to Chardron et al. [32], there are contradictory statements concerning adjusting the mcl-PHA MW by adapting to different fermentation conditions, such as pH. Thus, it is only strain-specific if HMW mcl-PHA is produced at low or high pH values.

Prospective studies should investigate whether the MW of mcl-PHAs is process-related using GPC as the method of choice. Unlike viscosity, which is also applied for MW determination, PDI might greatly determine the processing behavior together with M_w. This is due to the impact of both properties on the glass transition and melting point, which are essential factors for selecting conditions for processing biopolymers such as mcl-PHA.

5.4 | Analyzing the thermal properties

Differential scanning calorimetry (DSC) and Thermogravimetric analysis (TGA) are used to determine the thermal properties of elastomers and thermoplasts. The thermal characteristics are decisive considering the mechanical properties at a given temperature and are highly relevant for processing PHAs by extrusion, melt spinning, or injection molding. Furthermore, these characteristics greatly determine the respective application fields.

In this context, crystalline scl-PHA has typical thermoplastic properties, whereas mcl-PHA resins resemble elastomers and latex-like materials [92]. The low thermal stability of scl-PHAs limits their applicability and processibility because of a narrow processing window [93]. The glass transition temperature of scl-PHAs is near room temperature, indicating its high brittleness and secondary crystallization during storage. To overcome these limitations, nucleating agents and/or plasticizers need to be added for processing and application [94]. Combining scl- and mcl-PHAs has been shown to significantly improve thermal stability and compensate for the disadvantages of both PHAs [95]. The authors determined that the melting temperature T_m did not vary with the composition. However, a decrease in the crystallinity and crystallization temperature T_c could be confirmed by DSC. In addition, the decomposition temperature T_d increased for TGA after adding a higher amount of P3HO to P3HB.

5.4.1 | Decomposition temperature (T_d)

T_d defines the temperature at which a compound degrades under heating. The overall decomposition reaction, independent of the PHA type, involves the hydrolysis of ester linkages, resulting in LMW-PHAs. A small proportion of unsaturated side-chain fragments undergo oxidative cleavage at C C-linkages, producing a minor number of LMW esters and acids. The terminal hydroxyl group can undergo dehydration at higher temperatures to form an alkenoic acid [96]. Most mcl-PHAs with saturated monomers exhibit single-step degradation in the temperature range 255−350°C. Incorporating monomers with a longer alkyl chain has increased T_d [45, 53]. Razaif-Mazinah et al. [40] stated that a unique monomer distribution and shorter monomeric chain lengths resulted in a lower T_d. Still, the variation is only in a narrow range (275−283°C). This confirms that the T_d barely depends on the monomer composition, unlike the melting and glass transition temperatures.

5.4.2 | Melting temperature (T_m) and glass transition temperature (T_g) using DSC

The melting temperature T_m is an essential parameter for characterizing mcl-PHA. Melting peaks can be attributed to the melting of the crystalline regions in the polymer [43]. Based on previous studies, the median T_m value for mcl-PHAs was 47°C. However, the variations in the individual T_m were quite large. A significantly lower T_m of 15°C was reported by Cerrone et al. [33], while other studies reported much higher values, up to 173°C [45]. In this

case, the high T_m, similar to T_m of scl-PHAs, was attributed to increased side-chain crystallization of the long-chain monomers.

Several mcl-PHAs do not undergo melting or exhibit only a broad undefined peak in the commonly observed temperature region (30–120°C) [13, 25, 40, 81, 97]. Resultantly, the enthalpy changes were not recorded. This is because the mcl-PHAs produced are amorphous elastomers [98]. Further, the melting peak might depend on preliminary treatment. Studies showed that a 5-week-old mcl-PHA exhibits no melting peak in a second DSC measurement [61], whereas two T_m peaks are generally observed in mcl-PHAs [77].

A material's glass transition temperature (T_g) describes the temperature at which it transitions from a hard, brittle, glassy state to a viscous, rubbery state. At this temperature, the amorphous regions change from rigid to flexible. As the average T_g of mcl-PHAs is around −43°C, it is mainly in an amorphous state, exhibiting elastomeric behavior at room temperature [48]. The T_g of mcl-PHAs is lower than that for most polymers, such as nylon 6,6 (57°C), polycarbonate (150°C), or polyvinyl acetate (28°C) [99], and most scl-PHAs (around 0°C).

The T_g depends on the purity as residual contamination of PHA with the substrate results in a deviation from the expected T_g range, as reported by Cruz et al. [41]. In particular, compounds with cross-linking ability, such as triglycerides, increase the T_g due to reduced mobility of mcl-PHA [100].

The side-chain structure and chemical composition of the monomers determine both T_m and T_g. A comparison of previous data shows that T_g decreases with increasing monomer chain length [48, 101]. Abe et al. [101] stated that the T_m of solvent-cast films consisting of mcl-P(3HA)s decreased from 59°C to 45°C, changing the side-chain length from three P(3HHx) to four P(3HHp) carbon atoms. Extending the side-chain length of the mcl-PHA to seven carbon atoms as it is within P(3HD) increased the T_m to 69°C.

Other authors showed that the monomer distribution is a major impact factor. This is reflected by higher T_m and T_g values due to a less diverse monomer composition [33]. Abe et al. [101] argued that diversity in the monomer composition inhibits the formation of stable crystalline regions. This was confirmed by Li et al. [77] and Jiang et al. [102], who stated that a higher share of a dominant monomer increases T_m due to an increased melting enthalpy, of which the median of all investigated studies is about 16 J g^{-1}. These authors showed a positive linear relationship between the dominant monomer content and T_m. Therefore, it is not surprising that mcl-PHAs with a particular dominant monomer exhibit thermal properties similar to those of P3HD [63]. Low T_m and T_g values indicate the presence of highly flexible chains and a large free volume in the mcl-PHAs due to bulky pendant alkyl chains [61].

5.4.3 | Cold crystallization temperature (T_{cc})

The cool crystallization temperature (T_{cc}) is another parameter for characterizing elastomeric polymers with DSC. Based on previous reports, the median T_{cc} for mcl-PHA was determined to be 55°C, similar to that for scl-PHAs. T_{cc} is the temperature at which at least a part of the polymers crystallize within cooling and is consistently lower than T_m. The degree of crystallinity $\boldsymbol{X}_c$ anon is not calculated using T_{cc} but the melting enthalpy at T_m.

5.4.4 | Degree of crystallinity (X_c)

X_c greatly affects the mechanical properties and degradation time of mcl-PHAs [103]. The crystalline regions are formed when the main and side chains are assembled in ordered layers. The higher the crystallinity, the more brittle is the material, the less susceptible to modification, and the lower the end-of-life degradation rate [45]. In addition to using DSC to calculate the X_c with T_m, the X_c of PHAs can also be determined using FT-IR [104] and X-ray [105] investigations.

The X_c of P3HBs range between 60% and 80% [45]. The median X_c value of mcl-PHAs is 23%. One study determined even lower X_c values at 6% [41], indicating that mcl-PHAs are only partially crystalline and that the polymer has a higher proportion of amorphous regions, resulting in rubber- or latex-like characteristics [36]. This was also by van der Walle et al. [106], who characterized mcl-PHA as a "highly amorphous elastomer." Amorphous properties result from incorporating unsaturated or long-chain monomers, high monomer diversity, and the random ordering of the respective monomers that interfere and decrease the crystallinity [43, 107].

The crystallization of mcl-PHAs was also found to be time-dependent. A study showed that the crystallinity of P(3HO-3HD-3HDD) changed during storage within the first 5 weeks after its production. Guo et al. [107] incubated this polymer for 24 h at room temperature before measuring X_c via X-ray and showed that the crystallization process requires a long time [61]. Thus, the determination of Xc via DSC in the standard form is questionable because DSC includes heating and cooling of the sample in a short period; the Xc could differ from the one obtained by X-ray. Therefore, further investigations are required to compare X_c data obtained using X-ray and DSC as functions of different storage times. Precise values for

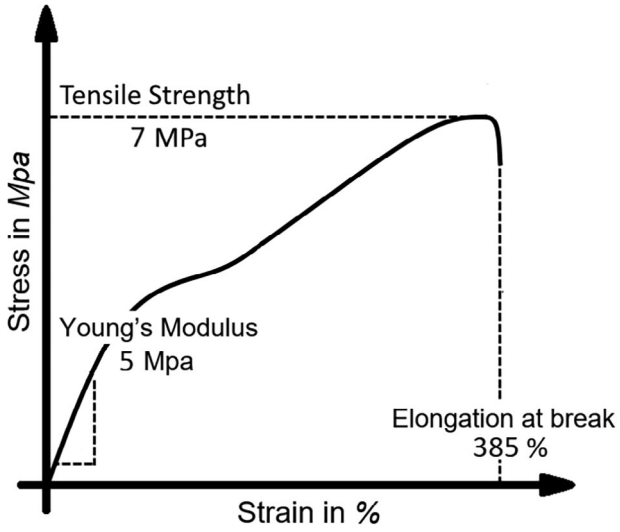

FIGURE 7 Schematic of a stress–strain curve with estimated median values for Young's modulus and elongation at break.

X_c are mandatory because they significantly impact the mechanical properties [108].

5.5 | Measuring mechanical properties

Although the investigations described above were still strongly oriented toward basic research, determining the mechanical properties of the mcl-PHAs using tensile testing machines is required for their application. The mechanical properties of a material are crucial for its processing behavior, which further determines its prospective applications. Objective analyses must evaluate properties such as brittleness, glassiness, and elasticity to characterize the material properly. The three main mechanical properties commonly measured for mcl-PHAs include elongation at break ε, tensile strength σ, and Young's modulus E. These are calculated using a tensile tester to measure the deformation and fracture of a specimen, resulting in a specific stress–strain curve (see Figure 7) with the respective data.

Generally, the value ranges determined for the mechanical tests are significant, based on the variability of the mcl-PHAs or due to challenges during the performance of the tests [108]. This holds especially true for ε, a measure of deformability under stress. For example, studies have shown that the ε values for mcl-PHAs vary greatly (ε = 20%–1384%). The median ε is at 385%, thus greatly exceeding the values commonly published for P3HB (ε = 2%) [109, 110]. It might be because the mcl-monomers foster the elasticity of the material [107]. Based on the ε values, mcl-PHA resins are considered to be elastomeric, similar to latex and rubber, making them suitable for soft tissue engineering applications [45].

Young's modulus E can be estimated as the slope of the elastic region in the stress–strain diagram (Figure 7). The previously reported E values were between 2 MPa [61] and 48 MPa [77]. As E is a function of the monomer chain length in mcl-PHA, the higher the average chain length of the monomers in mcl-PHA, the higher the E. The same holds when higher fractions of the dominant monomer are fed [102]. Both findings were confirmed by Ouyang et al. [85], who increased the share of 3HDD in the polymer. Similarly, Jiang et al. [102] observed an eightfold increase in E when the 3HN amount in the polymer was increased from 70% to 95%.

The local degree of order within the polymer and the arrangement of the monomers also affects the mechanical properties. The mechanical properties of two PHA polymers with the same composition, one with block-by-block and the other with random heterogeneous copolymer arrangements differ significantly [49].

The Storage (E‘) and Loss Modulus (E‘‘) can be measured by the apparent viscosity and viscoelastic properties Cruz et al. [41]. Thus, viscosity has been shown to significantly contribute to the mechanical behavior of mcl-PHA films at temperatures below T_m. The E‘ is significantly temperature dependent, exhibiting high values below T_g [43], corresponding to the material's stiffness. At room temperature, the E‘ of mcl-PHA is low, indicating that it is soft and elastic. Hence, evaluating the E‘ of mixtures of crystalline polymers can support processing in a standard extruder [43]. In addition, mcl-PHA was found to be an appropriate precursor for natural-based adhesives by subjecting the material to shear bond strength tests [41]. The E‘ of mcl-PHA has been shown to be greatly enhanced by adding Cloisite 15 A as a filler [32], probably attributed to a greater interfacial area between PHA and filler.

5.6 | Further mcl-PHA investigations

Most studies investigated the mcl-PHA characteristics using above-mentioned analytical instruments and methods. Based on our literature search, we also identified seldom-used analytical tools to characterize PHAs. As this additional data might help identify suitable applications, we would like to introduce them, in this section, briefly and comment on their suitability.

Contact angle tests can be used to evaluate the mechanical properties of mcl-PHA films. The results revealed that mcl-PHAs are inherently hydrophobic, exhibiting contact angle values between 88° and 101° [61, 111]. However, the authors state that this value has limited validity because the wettability is also influenced by the material roughness [61]. Furthermore, the value is too low for

the specific hydrophobicity of different materials, such as textiles.

Protein adsorption is essential for the biocompatibility and accessibility of the interaction surface of a material. It is a prerequisite to use PHAs in implants [114]. The protein adsorption was determined to be between 0.083 and 0.7 mg cm^{-2} [61, 112, 113]. Notably, hydrophobicity and protein adsorption are a function of the surface morphology, which can be assessed via scanning electron microscopy (SEM).

Although evaluating the material before application is crucial, values indicating the purity of the extracted PHAs are unavailable. Elemental analysis can be used to assess impurities derived from proteins by measuring the protein content via nitrogen amount [36], providing information regarding the purity. Further, it could also be used to reveal an "average" monomer chain length while measuring a pure sample [11]. However, the primary contamination in the mcl-PHAs is lipids, which cannot be determined using elemental analysis.

6 | CONCLUSION

While the production and application of microbially produced PHAs has been of research increasingly for several decades, its industrial implementation has only recently started gaining momentum. Scl-PHAs, such as P3HB or P3HB3HV copolymer are relatively well known, as evidenced by the numerous publications in this area. Several publications are available solely for P3HB compared with studies concerning all mcl-PHAs. Although the mcl-PHAs still occupy a niche, their diversity and longer chain monomers complement the scl-PHA portfolio with entirely different physical and functional properties and processability.

mcl-PHA have been mainly produced using *Pseudomonas* cultured in shake flasks on a pilot scale (650 L) [35]. *Pseudomonas* has shown high cell density fermentation up to 160 g L^{-1} [18] and PHA accumulation capacity up to 74% CDW [19]. Unfortunately, as this species is often associated with health risks, its application must be regulated, and various safety precautions must be taken. Even though the engineered strain is not the focus of this review, approaches to delete the genes responsible for the expression of toxins are suitable, and vice versa (the genes for PHA production could also be transferred to other nontoxic hosts) would be a possible solution to the underlying problem.

Further, as the substrate selection and feeding strategy (e.g., feeding length and rate) affect the PHA's chemical composition, they have an economic impact. Therefore, a systematic study—which should be conducted for each microorganism or at least with the leading producer, *P. putida*—correlating the feed with the monomer composition of mcl-PHA would develop a more defined and tunable product.

The DSP of mcl-PHA remains a bottleneck that needs to be addressed by developing more sustainable and green purification methods. Although biotechnological alternatives to solvent-based purification processes are already being explored, they are still in the early stages. Furthermore, no purification method enables the isolation and separation of "native" PHA (in its intracellular intact granular form). Therefore, systematically investigating sustainable methods and the effects of purification methods on the chemical–physical properties, of mcl-PHAs is crucial.

Further, the monomeric pattern of mcl-PHAs is poorly understood despite its essential role in determining polymer properties. This is also why polymers with the same composition do not always exhibit the same physiochemical properties. The thermal and mechanical behavior of the polymer dramatically differs in the heterogeneous and block-by-block distribution of the monomers. However, analyzing monomer distribution is challenging, and even new analytics need to be developed and require specialist knowledge.

The diversity of the mcl-PHA monomer and its composition primarily determine the polymer's thermal properties and crystallinity. Although studies have provided melting temperature and glass transition temperature values, an in-depth investigation is required to correlate the monomeric composition, especially the composition's heterogeneity, to the thermal properties. The same applies to the mechanical properties of the mcl-PHAs determined using a tensile tester. The available data regarding the processing and application of mcl-PHA is insufficient, which hinders the identification of further suitable application fields. Nevertheless, attempts have been made to apply mcl-PHAs in biomedical applications, such as tissue engineering or drug delivery, because of their rubber-like and viscoelastic properties. However, this review has already identified the challenges that must be overcome to move mcl-PHA beyond medical applications and toward widespread commercialization.

ACKNOWLEDGMENTS

We would like to thank the following organizations for their financial support through various projects: German Federal Ministry of Education and Research (BMBF): SusPackaging (Grant Agreement no. 031B0371A and 031B0371D), German Federal Ministry of Food and Agriculture (BMEL): BiPoTex (Grant Agreement no. 2221NR012B), Ministry of the Environment, Climate and Energy Management, Baden-Württemberg and the EU

Commission: KoalAplan (Grant Agreement no. 2076393). In addition, we thank Amira Oraby and Dr. Alexander Beck for their support and critical feedback during the preparation of this publication.

Open access funding enabled and organized by Projekt DEAL.

CONFLICT OF INTEREST STATEMENT

The authors declare no conflicts of interest.

DATA AVAILABILITY STATEMENT

Data are available on request from the authors.

ORCID

Thomas Hahn https://orcid.org/0000-0001-8428-0342
Pravesh Tamang https://orcid.org/0000-0002-5994-0254

REFERENCES

1. Lemoigne M. Produits de dehydration et de polymerisation de l'acide ß-oxobutyrique. *Bull Soc Chim Biol*. 1926;8:770-782.
2. Możejko-Ciesielska J, Kiewisz R. Bacterial polyhydroxyalkanoates: still fabulous? *Microbiol Res*. 2016;192:271-282.
3. Berezina N, Martelli S. Bio-based polymers and materials. *RSC Green Chem*. 2014;2014:1-28.
4. Steinbüchel A, Valentin HE. Diversity of bacterial polyhydroxyalkanoic acids. *FEMS Microbiol Lett*. 1995;128:219-228.
5. Licciardello G, Catara AF, Catara V. Production of polyhydroxyalkanoates and extracellular products using *Pseudomonas Corrugata* and *P. Mediterranea*: a review.*Bioengineering (Basel, Switzerland)*. 2019;6:1-13.
6. Joce C. *PHA: Plastic the Way Nature Intended?* Cambridge Consultants; 2018.
7. Singh AK, Mallick N. Enhanced production of SCL-LCL-PHA co-polymer by sludge-isolated *Pseudomonas aeruginosa* MTCC 7925. *Lett Appl Microbiol*. 2008;46:350-357.
8. Singh AK, Mallick N. SCL-LCL-PHA copolymer production by a local isolate, *Pseudomonas aeruginosa* MTCC 7925. *Biotechnol J*. 2009;4:703-711.
9. Reddy VUN, Ramanaiah SV, Reddy MV, Chang YC. Review of the developments of bacterial medium-chain-length polyhydroxyalkanoates (mcl-PHAs). *Bioengineering (Basel)*. 2022;102:393-407.
10. Silva JB, Pereira JR, Marreiros BC, et al. Microbial production of medium-chain length polyhydroxyalkanoates. *Process Biochem*. 2021;102:393-407.
11. de Smet MJ, Eggink G, Witholt B, et al. Characterization of intracellular inclusions formed by *Pseudomonas oleovorans* during growth on octane. *J Bacteriol*. 1983;154:870-878.
12. Poblete-Castro I, Rodriguez AL, Lam CMC, Kessler W. Improved production of medium-chain-length polyhydroxyalkanoates in glucose-based fed-batch cultivations of metabolically engineered *Pseudomonas putida* strains. *J Microbiol Biotechnol*. 2014;24:59-69.
13. Ruiz C, Kenny ST, Narancic T, et al. Conversion of waste cooking oil into medium chain polyhydroxyalkanoates in a high cell density fermentation. *J Biotechnol*. 2019;306:9-15.
14. Diniz SC, Taciro MK, Cabrera Gomez JG, Pradella JGDC. High-Cell-Density cultivation of *Pseudomonas putida* IPT 046 and medium-chain-length polyhydroxyalkanoate production from sugarcane carbohydrates. *Appl Biochem Biotechnol*. 2004;119:51-69.
15. Blunt W, Dartiailh C, Sparling R, et al. Development of high cell density cultivation strategies for improved medium chain length polyhydroxyalkanoate productivity using *Pseudomonas putida* LS46. *Bioengineering (Basel, Switzerland)*. 2019;6:1-15.
16. Allen AD, Daley P, Ayorinde FO, et al. Characterization of medium chain length (R)-3-hydroxycarboxylic acids produced by *Streptomyces* sp. JM3 and the evaluation of their antimicrobial properties. *World J Microbiol Biotechnol*. 2012;28:2791-2800.
17. Wecker P, Moppert X, Simon-Colin C, et al. Discovery of a mcl-PHA with unexpected biotechnical properties: the marine environment of French Polynesia as a source for PHA-producing bacteria. *AMB Express*. 2015;5:74-74.
18. Ruiz C, Kenny ST, Babu PR, et al. High cell density conversion of hydrolysed waste cooking oil fatty acids into medium chain length polyhydroxyalkanoate using *Pseudomonas putida* KT2440. *Catalysts*. 2019;9:14.
19. Gao J, Ramsay JA, Ramsay BA. Fed-batch production of poly-3-hydroxydecanoate from decanoic acid. *J Biotechnol*. 2016;218:102-107.
20. Choonut A, Prasertsan P, Klomklao S, Sangkharak K. Study on mcl-PHA production by novel thermotolerant gram-positive isolate. *J Polym Environ*. 2020;28:2410-2421.
21. Satoh Y, Tajima K, Nakamoto S, et al. Isolation of a thermotolerant bacterium producing medium-chain-length polyhydroxyalkanoate. *J Appl Microbiol*. 2011;111:811-817.
22. Sun Z, Ramsay J, Guay M, Ramsay B. Enhanced yield of medium-chain-length polyhydroxyalkanoates from nonanoic acid by co-feeding glucose in carbon-limited, fed-batch culture. *J Biotechnol*. 2009;143:262-267.
23. Sun Z, Ramsay JA, Guay M, Ramsay BA. Fed-batch production of unsaturated medium-chain-length polyhydroxyalkanoates with controlled composition by *Pseudomonas putida* KT2440. *Appl Microbiol Biotechnol*. 2009;82:657-662.
24. Li Y, Yang S, Jin D, Jia X. Optimization of medium-chain-length polyhydroxyalkanoate production by *Pseudomonas putida* KT2440 from co-metabolism of glycerol and octanoate. *Can J Chem Eng*. 2021;99:657-666.
25. Follonier S, Riesen R, Zinn M. Pilot-scale production of functionalized mcl-PHA from grape pomace supplemented with fatty acids. *Chem Biochem Eng Q*. 2015;29:113-121.
26. Borrero-de Acuna JM, Aravena-Carrasco C, Gutierrez-Urrutia I, et al. Enhanced synthesis of medium-chain-length poly(3-hydroxyalkanoates) by inactivating the tricarboxylate transport system of *Pseudomonas putida* KT2440 and process development using waste vegetable oil. *Process Biochem*. 2019;77:23-30.
27. Andin N, Longieras A, Veronese T, et al. Improving carbon and energy distribution by coupling growth and medium chain length polyhydroxyalkanoate production from fatty acids by *Pseudomonas putida* KT2440. *Biotechnol Bioprocess Eng*. 2017;22:308-318.
28. Shang L, Jiang M, Yun Z, et al. Mass production of medium-chain-length poly(3-hydroxyalkanoates) from hydrolyzed corn oil by fed-batch culture of *Pseudomonas putida*. *World J Microbiol Biotechnol*. 2008;24:2783-2787.

29. Hrncirik P, Nahlik J, Mares J. Strategies for automated control of the bioproduction of McI-PHA biopolymers. *Chem Biochem Eng Q*. 2017;31:241-250.
30. Kellerhals MB, Hazenberg W, Witholt B. High cell density fermentations of *Pseudomonas oleovorans* for the production of mcl-PHAs in two-liquid phase media. *Enzyme Microb Technol*. 1999;24:111-116.
31. Jung K, Hazenberg W, Prieto M, Witholt B. Two-stage continuous process development for the production of medium-chain-length poly(3-hydroxyalkanoates). *Biotechnol Bioeng*. 2001;72:19-24.
32. Chardron S, Bruzaud S, Lignot B, et al. Characterization of bionanocomposites based on medium chain length polyhydroxyalkanoates synthesized by *Pseudomonas oleovorans*. *Polym Test*. 2010;29:966-971.
33. Cerrone F, Duane G, Casey E, et al. Fed-batch strategies using butyrate for high cell density cultivation of *Pseudomonas putida* and its use as a biocatalyst. *Appl Microbiol Biotechnol*. 2014;98:9217-9228.
34. Muhr A, Rechberger EM, Salerno A, et al. Novel description of mcl-PHA biosynthesis by *Pseudomonas chlororaphis* from animal-derived waste. *J Biotechnol*. 2013;165:45-51.
35. Elbahloul Y, Steinbüchel A. Large-scale production of poly(3-hydroxyoctanoic acid) by *Pseudomonas putida* GPo1 and a simplified downstream process. *Appl Environ Microbiol*. 2009;75:643-651.
36. Muhr A, Rechberger EM, Salerno A, et al. Biodegradable latexes from animal-derived waste: biosynthesis and characterization of mcl-PHA accumulated by *Ps. citronellolis*. *React Funct Polym*. 2013;73:1391-1398.
37. Blunt W, Dartiailh C, Sparling R, et al. Microaerophilic environments improve the productivity of medium chain length polyhydroxyalkanoate biosynthesis from fatty acids in *Pseudomonas putida* LS46. *Process Biochem*. 2017;59:18-25.
38. Kenny ST, Runic JN, Kaminsky W, et al. Development of a bioprocess to convert PET derived terephthalic acid and biodiesel derived glycerol to medium chain length polyhydroxyalkanoate. *Appl Microbiol Biotechnol*. 2012;95:623-633.
39. Munawar KMM, Simarani K, Annuar MSM. Bioconversion of mixed free fatty acids to poly-3-hydroxyalkanoates by *Pseudomonas putida* BET001 and modeling of its fermentation in shake flasks. *Electron J Biotechnol*. 2016;19:50-55.
40. Razaif-Mazinah MRM, Annuar MSM, Sharifuddin Y. Effects of even and odd number fatty acids cofeeding on PHA production and composition in *Pseudomonas putida* Bet001 isolated from palm oil mill effluent. *Biotechnol Appl Biochem*. 2016;63:92-100.
41. Cruz MV, Araújo D, Alves VD, et al. Characterization of medium chain length polyhydroxyalkanoate produced from olive oil deodorizer distillate. *Int J Biol Macromol*. 2016;82:243-248.
42. Follonier S, Goyder MS, Silvestri A-C, et al. Fruit pomace and waste frying oil as sustainable resources for the bioproduction of medium-chain-length polyhydroxyalkanoates. *Int J Biol Macromol*. 2014;71:42-52.
43. Urbina L, Wongsirichot P, Corcuera MA, et al. Application of cider by-products for medium chain length polyhydroxyalkanoate production by *Pseudomonas putida* KT2440. *Eur Polym J*. 2018;108:1-9.
44. Wongsirichot P, Gonzalez-Miquel M, Winterburn J. Holistic valorization of rapeseed meal utilizing green solvents extraction and biopolymer production with *Pseudomonas putida*. *J Clean Prod*. 2019;230:420-429.
45. Sathiyanarayanan G, Bhatia SK, Song H-S, et al. Production and characterization of medium-chain-length polyhydroxyalkanoate copolymer from Arctic psychrotrophic bacterium *Pseudomonas* sp. PAMC 28620. *Int J Biol Macromol*. 2017;97:710-720.
46. Sangkharak K, Paichid N, Yunu T, et al. Utilisation of tuna condensate waste from the canning industry as a novel substrate for polyhydroxyalkanoate production. *Biomass Convers Biorefin*. 2020;11:2053-2064.
47. Możejko J, Ciesielski S. Pulsed feeding strategy is more favorable to medium-chain-length polyhydroxyalkanoates production from waste rapeseed oil. *Biotechnol Prog*. 2014;30:1243-1246.
48. Możejko J, Ciesielski S. Saponified waste palm oil as an attractive renewable resource for mcl-polyhydroxyalkanoate synthesis. *J Biosci Bioeng*. 2013;116:485-492.
49. Tripathi L, Wu L-P, Dechuan M, et al. *Pseudomonas putida* KT2442 as a platform for the biosynthesis of polyhydroxyalkanoates with adjustable monomer contents and compositions. *Bioresour Technol*. 2013;142:225-231.
50. Hanik N, Utsunomia C, Arai S, et al. Influence of unusual co-substrates on the biosynthesis of medium-chain-length polyhydroxyalkanoates produced in multistage chemostat. *Front Bioeng Biotechnol*. 2019;7:9.
51. Liu MH, Chen YJ, Lee CY. Characterization of medium-chain-length polyhydroxyalkanoate biosynthesis by *Pseudomonas mosselii* TO7 using crude glycerol. *Biosci Biotechnol Biochem*. 2018;82:532-539.
52. Kang DK, Lee CR, Lee SH, et al. Production of polyhydroxyalkanoates from sludge palm oil using *Pseudomonas putida* S12. *J Microbiol Biotechnol*. 2017;27:990-994.
53. Gumel AM, Annuar MSM, Heidelberg T. Biosynthesis and characterization of polyhydroxyalkanoates copolymers produced by *Pseudomonas putida* Bet001 isolated from palm oil mill effluent. *PLOS ONE*. 2012;7:e45214.
54. Liu S, Narancic T, Tham J-L, O'Connor KE. β-oxidation–polyhydroxyalkanoates synthesis relationship in *Pseudomonas putida* KT2440 revisited. *Appl Microbiol Biotechnol*. 2023;107:1863-1874.
55. Tian WD, Hong K, Chen GQ, et al. Production of polyesters consisting of medium chain length 3-hydroxyalkanoic acids by *Pseudomonas mendocina* 0806 from various carbon sources. *Antonie Van Leeuwenhoek*. 2000;77:31-36.
56. Yang X, Li S, Jia X. A four-microorganism three-step fermentation process for producing medium-chain-length polyhydroxyalkanoate from starch. *3 Biotech*. 2020;10:352.
57. Sharma PK, Fu J, Cicek N, et al. Kinetics of medium-chain-length polyhydroxyalkanoate production by a novel isolate of *Pseudomonas putida* LS46. *Can J Microbiol*. 2012;58:982-989.
58. Choonut A, Prasertsan P, Klomklao S, Sangkharak K. *Bacillus thermoamylovorans*-related strain isolated from high temperature sites as potential producers of medium-chain-length polyhydroxyalkanoate (mcl-PHA). *Curr Microbiol*. 2020;77:3044-3056.

59. Vastano M, Corrado I, Sannia G, et al. Conversion of no/low value waste frying oils into biodiesel and polyhydroxyalkanoates. *Sci Rep*. 2019;9:8.
60. Lee SY, Wong HH, Choi J-I, et al. Production of medium-chain-length polyhydroxyalkanoates by high-cell-density cultivation of *Pseudomonas putida* under phosphorus limitation. *Biotechnol Bioeng*. 2000;68:466-470.
61. Basnett P, Marcello E, Lukasiewicz B, et al. Biosynthesis and characterization of a novel, biocompatible medium chain length polyhydroxyalkanoate by *Pseudomonas mendocina* CH50 using coconut oil as the carbon source. *J Mater Sci Mater Med*. 2018;29:179.
62. Davis R, Kataria R, Cerrone F, et al. Conversion of grass biomass into fermentable sugars and its utilization for medium chain length polyhydroxyalkanoate (mcl-PHA) production by *Pseudomonas* strains. *Bioresour Technol*. 2013;150:202-209.
63. Liu Y, Yang S, Jia X. Construction of a "nutrition supply–detoxification" coculture consortium for medium-chain-length polyhydroxyalkanoate production with a glucose–xylose mixture. *J Ind Microbiol Biotechnol*. 2020;47:343-354.
64. Sangkharak K, Choonut A, Rakkan T, Prasertsan P. The degradation of phenanthrene, pyrene, and fluoranthene and its conversion into medium-chain-length polyhydroxyalkanoate by novel polycyclic aromatic hydrocarbon-degrading bacteria. *Curr Microbiol*. 2020;77:897-909.
65. Yasotha K, Aroua MK, Ramachandran KB, Tan IKP. Recovery of medium-chain-length polyhydroxyalkanoates (PHAs) through enzymatic digestion treatments and ultrafiltration. *Biochem Eng J*. 2006;30:260-268.
66. Heinrich D, Madkour MH, Al-Ghamdi MA, et al. Large scale extraction of poly(3-hydroxybutyrate) from *Ralstonia eutropha* H16 using sodium hypochlorite. *AMB Express*. 2012;2:59.
67. Jiang X, Ramsay JA, Ramsay BA. Acetone extraction of mcl-PHA from *Pseudomonas putida* KT2440. *J Microbiol Methods*. 2006;67:212-219.
68. Mondal S, Syed UT, Gil C, et al. A novel sustainable PHA downstream method. *Green Chem*. 2023;25:1137-1149.
69. Kathiraser Y, Aroua MK, Ramachandran KB, Tan IKP. Chemical characterization of medium-chain-length polyhydroxyalkanoates (PHAs) recovered by enzymatic treatment and ultrafiltration. *J Chem Technol Biotechnol*. 2007;82:847-855.
70. Pagliano G, Galletti P, Samorì C, et al. Recovery of polyhydroxyalkanoates from single and mixed microbial cultures: a review. *Front Bioeng Biotechnol*. 2021;9:1-28.
71. Jiang Y, Mikova G, Kleerebezem R, et al. Feasibility study of an alkaline-based chemical treatment for the purification of polyhydroxybutyrate produced by a mixed enriched culture. *AMB Express*. 2015;5:5.
72. Yeol Lee E, Yong Choi C. Structural identification of polyhydroxyalkanoic acid (PHA) containing 4-hydroxyalkanoic acids by gas chromatography-mass spectrometry (GC-MS) and its application to bacteria screening. *Biotechnol Tech*. 1997;11:167-171.
73. Mohammadi M, Hassan M, Yee P, et al. Efficient polyhydroxyalkanoate recovery from recombinant *Cupriavidus necator* by using low concentration of NaOH. *Environ Eng Sci*. 2012;29:783-789.
74. Furrer P, Hany R, Rentsch D, et al. Quantitative analysis of bacterial medium-chain-length poly([R]-3-hydroxyalkanoates) by gas chromatography. *J Chromatogr*. 2007;1143:199-206.
75. Hong K, Sun S, Tian W, et al. A rapid method for detecting bacterial polyhydroxyalkanoates in intact cells by Fourier transform infrared spectroscopy. *Appl Microbiol Biotechnol*. 1999;51:523-526.
76. Simon-Colin C, Alain K, Raguénès G, et al. Biosynthesis of medium chain length poly(3-hydroxyalkanoates) (mcl PHAs) from cosmetic co-products by *Pseudomonas raguenesii* sp. nov., isolated from Tetiaroa, French Polynesia. *Bioresour Technol*. 2009;100:6033-6039.
77. Li H-L, Deng R-X, Wang W, et al. Biosynthesis and characterization of medium-chain-length polyhydroxyalkanoate with an enriched 3-hydroxydodecanoate monomer from a *Pseudomonas chlororaphis* cell factory. *J Agric Food Chem*. 2021;69:3895-3903.
78. Huang P, Okoshi T, Mizuno S, et al. Gas chromatography-mass spectrometry-based monomer composition analysis of medium-chain-length polyhydroxyalkanoates biosynthesized by *Pseudomonas* spp. *Biosci, Biotechnol, Biochem*. 2018;82:1615-1623.
79. de Waard P, van der Wal H, Huijberts GN, Eggink G. Heteronuclear NMR analysis of unsaturated fatty acids in poly(3-hydroxyalkanoates). Study of beta-oxidation in *Pseudomonas putida*. *J Biol Chem*. 1993;268:315-319.
80. Linton E, Rahman A, Viamajala S, et al. Polyhydroxyalkanoate quantification in organic wastes and pure cultures using a single-step extraction and 1H NMR analysis. *Water Sci Technol*. 2012;66:1000-1006.
81. Haba E, Vidal-Mas J, Bassas M, et al. Poly 3-(hydroxyalkanoates) produced from oily substrates by *Pseudomonas aeruginosa* 47T2 (NCBIM 40044): effect of nutrients and incubation temperature on polymer composition. *Biochem Eng J*. 2007;35:99-106.
82. Choi T-R, Park Y-L, Song H-S, et al. Fructose-based production of short-chain-length and medium-chain-length polyhydroxyalkanoate copolymer by arctic *Pseudomonas* sp. B14-6. *Polymers*. 2021;13:1398.
83. Hong S-G, Hsu H-W, Ye M-T. Thermal properties and applications of low molecular weight polyhydroxybutyrate. *J Therm Anal Calorim*. 2013;111:1243-1250.
84. Ni Y-Y, Kim DY, Chung MG, et al. Biosynthesis of medium-chain-length poly(3-hydroxyalkanoates) by volatile aromatic hydrocarbons-degrading *Pseudomonas fulva* TY16. *Bioresour Technol*. 2010;101:8485-8488.
85. Ouyang S-P, Luo RC, Chen S-S, et al. Production of polyhydroxyalkanoates with high 3-hydroxydodecanoate monomer content by fadB and fadA knockout mutant of *Pseudomonas putida* KT2442. *Biomacromolecules*. 2007;8:2504-2511.
86. Nikodinovic J, Kenny ST, Babu RP, et al. The conversion of BTEX compounds by single and defined mixed cultures to medium-chain-length polyhydroxyalkanoate. *Appl Microbiol Biotechnol*. 2008;80:665-673.
87. Tsuge T. Fundamental factors determining the molecular weight of polyhydroxyalkanoate during biosynthesis. *Polym J*. 2016;48:1051-1057.

88. Zinn M, Witholt B, Egli T. Occurrence, synthesis and medical application of bacterial polyhydroxyalkanoate. *Adv Drug Del Rev*. 2001;53:5-21.
89. Walsh M, O'Connor K, Babu R, et al. Plant oils and products of their hydrolysis as substrates for polyhydroxyalkanoate synthesis. *Chem Biochem Eng Q*. 2015;29:123-133.
90. Bartels M, Gutschmann B, Widmer T, et al. Recovery of the PHA copolymer P(HB-co-HHx) with non-halogenated solvents: influences on molecular weight and HHx-Content. *Front Bioeng Biotechnol*. 2020;8:12.
91. Wampfler B, Ramsauer T, Rezzonico S, et al. Isolation and purification of medium chain length poly(3-hydroxyalkanoates) (mcl-PHA) for medical applications using nonchlorinated solvents. *Biomacromolecules*. 2010;11:2716-2723.
92. Koller M, Maršálek L, de Sousa Dias MM, Braunegg G. Producing microbial polyhydroxyalkanoate (PHA) biopolyesters in a sustainable manner. *New Biotechnol*. 2017;37:24-38.
93. Larsson M, Markbo O, Jannasch P. Melt processability and thermomechanical properties of blends based on polyhydroxyalkanoates and poly(butylene adipate-co-terephthalate). *RSC Adv*. 2016;6:44354-44363.
94. Bugnicourt E, Cinelli P, Alvarez V, Lazzeri A. Polyhydroxyalkanoate (PHA): review of synthesis, characteristics, processing and potential applications in packaging. *Express Polym Lett*. 2014;8:791-808.
95. Nerkar M, Ramsay JA, Ramsay BA, Kontopoulou M. Melt compounded blends of short and medium chain-length poly-3-hydroxyalkanoates. *J Environ Polym*. 2014;22:236-243.
96. Sin MC, Gan SN, Annuar MSM, Tan IKP. Thermodegradation of medium-chain-length poly(3-hydroxyalkanoates) produced by *Pseudomonas putida* from oleic acid. *Polym Degradation Stab*. 2010;95:2334-2342.
97. Kato M, Bao HJ, Kang C-K, et al. Production of a novel copolyester of 3-hydroxybutyric acid and medium-chain-length 3-hydroxyalkanoic acids by *Pseudomonas* sp. 61-3 from sugars. *Appl Microbiol Biotechnol*. 1996;45:363-370.
98. Chan Sin M, Gan SN, Mohd Annuar MS, Ping Tan IK. Thermodegradation of medium-chain-length poly(3-hydroxyalkanoates) produced by *Pseudomonas putida* from oleic acid. *Polym Degradation Stab*. 2010;95:2334-2342.
99. Balani K, Verma V, Agarwal A, Narayan R. Physical, thermal, and mechanical properties of polymers. In: Balani K, Verma V, Agarwal A, Narayan R, ed. *Biosurfaces: A Materials Science and Engineering Perspective*. John Wiley & Sons, Inc.; 2014:329-344.
100. Laycock B, Halley P, Pratt S, et al. The chemomechanical properties of microbial polyhydroxyalkanoates. *Prog Polym Sci*. 2014;39:397-442.
101. Abe H, Ishii N, Sato S, Tsuge T. Thermal properties and crystallization behaviors of medium-chain-length poly(3-hydroxyalkanoate)s. *Polymer*. 2012;53:3026-3034.
102. Jiang X, Sun Z, Marchessault RH, et al. Biosynthesis and properties of medium-chain-length polyhydroxyalkanoates with enriched content of the dominant monomer. *Biomacromolecules*. 2012;13:2926-2932.
103. Larrañaga A, Fernández J, Vega A, et al. Crystallization and its effect on the mechanical properties of a medium chain length polyhydroxyalkanoate. *J Mech Behav Biomed Mater*. 2014;39:87-94.
104. Kansiz M, Domínguez-Vidal A, McNaughton D, Lendl B. Fourier-transform infrared (FTIR) spectroscopy for monitoring and determining the degree of crystallisation of polyhydroxyalkanoates (PHAs). *Anal Bioanal Chem*. 2007;388:1207-1213.
105. Volova T, Zhila N, Shishatskaya E, et al. The physicochemical properties of polyhydroxyalkanoates with different chemical structures. *Polym Sci Ser A*. 2013:55.
106. van der Walle GAM, Buisman GJH, Weusthuis RA, Eggink G. Development of environmentally friendly coatings and paints using medium-chain-length poly(3-hydroxyalkanoates) as the polymer binder. *Int J Biol Macromol*. 1999;25:123-128.
107. Guo WB, Song CJ, Kong MM, et al. Simultaneous production and characterization of medium-chain-length polyhydroxyalkanoates and alginate oligosaccharides by *Pseudomonas mendocina* NK-01. *Appl Microbiol Biotechnol*. 2011;92:791-801.
108. Dartiailh C, Blunt W, Sharma PK, et al. The Thermal and mechanical properties of medium chain-length polyhydroxyalkanoates produced by *Pseudomonas putida* LS46 on various substrates. *Front Bioeng Biotechnol*. 2021:8.
109. Schmid MT, Sykacek E, O'Connor K, et al. Pilot scale production and evaluation of mechanical and thermal properties of P(3HB) from *Bacillus megaterium* cultivated on desugarized sugar beet molasses. *J Appl Polym Sci*. 2022;139:51503.
110. Stanley A, Murthy PSK, Vijayendra SVN. Characterization of polyhydroxyalkanoate produced by *Halomonas venusta* KT832796. *J Environ Polym*. 2020;28:973-983.
111. Bagdadi AV, Safari M, Dubey P, et al. Poly(3-hydroxyoctanoate), a promising new material for cardiac tissue engineering. *J Tissue Eng Regen Med*. 2018;12:e495-e512.
112. Rai R, Roether JA, Knowles JC, et al. Highly elastomeric poly(3-hydroxyoctanoate) based natural polymer composite for enhanced keratinocyte regeneration. *Int J Polym Mater*. 2017;66:326-335.
113. Chung MG, Kim HW, Kim BR, et al. Biocompatibility and antimicrobial activity of poly(3-hydroxyoctanoate) grafted with vinylimidazole. *Int J Biol Macromol*. 2012;50:310-316.
114. Rechendorff K, Hovgaard MB, Foss M, et al. Enhancement of protein adsorption induced by surface roughness. *Langmuir*. 2006;22:10885-10888.

How to cite this article: Hahn T, Alzate MO, Leonhardt S, Tamang P, Zibek S. Current trends in medium-chain-length polyhydroxyalkanoates: Microbial production, purification, and characterization. *Eng Life Sci*. 2024;24:e2300211. https://doi.org/10.1002/elsc.202300211